

Cite this: *Dalton Trans.*, 2021, **50**, 10947

Homoleptic quasilinear metal(I/II) silylamides of Cr–Co with phenyl and allyl functions – impact of the oxidation state on secondary ligand interactions†

Ruth Weller, Lutz Ruppach, Alena Shlyaykher, Frank Tambornino  and C. Gunnar Werncke *

Herein we describe the synthesis and characterization of a variety of new quasilinear metal(I/II) silylamides of the type $[M(N(Dipp)SiR_3)_2]^{0-}$ ($M = Cr-Co$) with different silyl substituents ($SiR_3 = SiPh_{3-n}Me_n$ ($n = 1-3$), $SiMe_2(allyl)$). By comparison of the solid state structures we show that in the case of phenyl substituents secondary metal–ligand interactions are suppressed upon reduction of the metal. Introduction of an allyl substituted silylamide gives divalent complexes with additional metal– π -alkene interactions with only weak activation of the $C=C$ bond but substantial bending of the principal $N-M-N$ axis. $1e^-$ -reduction makes cobalt a more strongly bound alkene substituent, whereas for chromium, reduction and intermolecular dimerisation of the allyl unit are observed. It thus indicates that the general view of low-coordinate 3d-metal ions as electron deficient seems not to apply to anionic metal(I) complexes. Additionally, the obtained cobalt(I) complexes are reacted with an aryl azide giving trigonal imido metal complexes. These can be regarded as rare examples of high-spin imido cobalt compounds from their structural and solution magnetic features.

Received 12th May 2021.

Accepted 7th July 2021

DOI: 10.1039/d1dt01543e

rsc.li/dalton

Introduction

Open-shell, linear complexes $[ML_2]$ are a rare class in coordination chemistry, which show promise in the fields of (catalytic) bond and element activation as well as molecular magnetism.^{1–3,4–10} These complexes are mostly found in the +II oxidation state bearing bulky anionic ligands such as amides,^{11,12} (thio)phenolates,^{6,13–15} or terphenyls.^{8,9,13,16} The steric encumbrance of the ligands shields the sterically and coordinatively unsaturated metal, and by that prevent dimerisation.¹⁷ A common trait in linear compounds are secondary interactions between the unsaturated metal ion and ligand substituents. This is especially prevalent for adjacent phenyl groups and leads to bending of the ligand–metal–ligand axis.^{1,2,4,6,13,15,18–21} While these interactions shield and stabilize the metal centre, they are unwanted in the case of molecule magnetism due to quenching of orbital angular momentum.^{4,9,12,20,22–24}

In the case of open-shell monovalent compounds, which are less numerous, the situation is less clear. For neutral linear metal(I) compounds, interactions of aryl substituents with the electron richer metal(I) are observable, as for example for mixed ligated NHC/amide or amidate nickel(I) compounds.^{18,19,25–27} Similarly, cationic complexes such as $[M(NHC)_2]^+$ give also evidence of an unsaturated metal ion *via* adduct formation, such as by THF or additional NHCs.²⁸ In contrast, for *anionic* linear metal(I) complexes $[ML_2]^-$, which are obtained by the reduction of the aforementioned $[ML_2]$ compounds, substantial metal–ligand interactions were so far not observed.^{5,7,10,29–31} Moreover, a singular report on the chromium complex $[Cr(N(Dipp)Si^iPr_3)_2]^{0-}$ (Dipp = 2,6-di-isopropylphenyl) hints at distinct differences with respect to the oxidation state, whereas only in the divalent case secondary ligand interactions are observed *via* pronounced bending of the Dipp moiety towards the metal ion (Fig. 1).²⁹

Recent reports by us and others concerning the behaviour of two-coordinate metal(I) ions bearing two anionic silylamide ligands also indicated a diverging behaviour of the metal(I) ion and an indifference of a two-coordinate metal(I) ion in $[ML_2]^-$ towards σ -donor ligands,^{6,30,32} that contrasts the situation of their divalent counterparts.^{33,34} Interactions of $[ML_2]^-$ with substrates were only observed if π -backbonding with or even formal $1e^-$ reduction of the substrate was possible.³⁵

Fachbereich Chemie, Philipps-Universität Marburg, Hans-Meerwein-Straße 4, D-35032 Marburg, Germany. E-mail: gunnar.werncke@chemie.uni-marburg.de

† Electronic supplementary information (ESI) available. CCDC 2073678–2073682, 2074223–2074237, 2074256 and 2074317. For ESI and crystallographic data in CIF or other electronic format see DOI: 10.1039/d1dt01543e

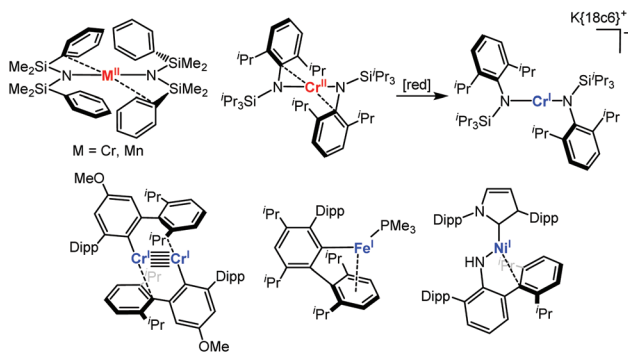


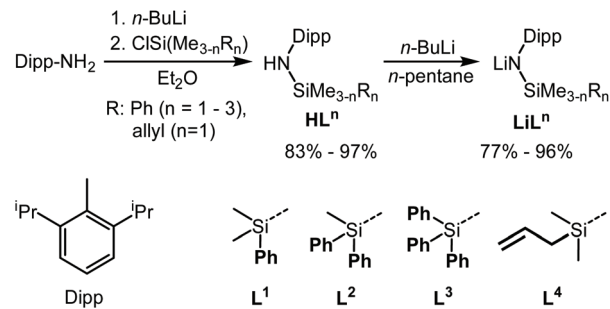
Fig. 1 Examples of low-coordinate metal(i/ii) complexes with secondary metal–ligand interactions (Dipp = 2,6-di-iso-propylphenyl).^{18,19,25,27,29}

Furthermore, in the case of formally neutral metal amides with intramolecular counter ion complexation ($[\text{KM}(\text{N}(\text{Dipp})\text{SiR}_3)_2]$), donor ligands exclusively coordinate to the counter ion, but not to the transition metal.³⁶ This evoked the question of the apparent lack of Lewis acidity of the 3d-metal(i) ion in these anionic compounds is an intrinsic feature or rather due to the absence of conformationally accessible arenes or other functionalities. In our general quest to broaden the usability of linear metal(i) silylamides, we aimed at the deliberate introduction of functionalities in quasilinear metal(i) complexes. This stems in part from their use as platforms for unusual metal–multiple bonds, which was recently shown for imido cobalt complexes.^{37,38}

In this report we present the synthesis of quasilinear metal(ii) bis(silylamide) complexes $[\text{ML}_2]$ ($\text{M} = \text{Cr}–\text{Co}$) bearing a $-\text{N}(\text{Dipp})\text{SiMe}_2\text{Ph}$ ligand ($=\text{L}^1$), with a coordinatively accessible phenyl function. In the solid state, these complexes show arene–metal interactions expectantly, which also exist in non-coordinating solvents. For chromium this is extended to $-\text{N}(\text{Dipp})\text{SiMePh}_2$ (L^2), and for iron to $-\text{N}(\text{Dipp})\text{SiPh}_3$ (L^3). Reduction of these complexes leads to anionic metal(i) complexes of type $\text{K}\{18\text{c}6\}[\text{ML}_2]$ (L^1 : Fe, Co; L^2 : Fe), in which such secondary metal–arene interactions are absent, and for manganese, intramolecular C–H activation is observed. This is extended to allyl substituents ($-\text{N}(\text{Dipp})\text{SiMe}_2(\text{allyl})$, L^4), in which the metal–alkene interaction is substantially stronger in the reduced state. In the case of chromium, one-electron reduction of the allyl function under concomitant Cr–C and intermolecular C–C bond formation is observed. For cobalt, the obtained monovalent compounds are used to obtain some additional rare imido cobalt complexes, which is remarkable in the presence of an allyl unit.

Results and discussion

The synthesis of homoleptic, linear metal(i) complexes bearing anionic ligands is, thus far, restricted to silylamide ligands such as $-\text{N}(\text{Dipp})\text{SiMe}_3$,^{6,7} $-\text{N}(\text{Dipp})\text{Si}^i\text{Pr}_3$ ²⁹ and $-\text{N}(\text{SiMe}_3)_2$ ⁷ or the silylmethanide $-\text{C}(\text{SiMe}_3)_3$.^{5,10} In these compounds sec-



Scheme 1 Synthetic pathway to the used lithio silylamides.

ondary interactions are absent likely due to steric reasons and lack of suitable functionalities. This holds also true for their direct divalent counterparts, with the exception of $[\text{Cr}(\text{N}(\text{Dipp})\text{Si}^i\text{Pr}_3)_2]$ (Fig. 1). As such, we sought to modify the $-\text{N}(\text{Dipp})\text{SiR}_3$ ligand sets accordingly by installing accessible phenyl functions ($\text{SiMe}_{3-n}\text{Ph}_n$, $n = 1–3$) at the Si atom. All aryl(silyl) amines were obtained by reacting stoichiometric amounts of 2,6-di-iso-propyl aniline with *n*-butyl lithium at -20°C followed by chlorosilane addition (Scheme 1).^{39,40} Work-up gave the amines as colourless oils ($\text{HN}(\text{Dipp})\text{SiMe}_{3-n}\text{Ph}_n$: HL^1 ($n = 1$), HL^2 ($n = 2$)) or as white solids ($\text{HN}(\text{Dipp})\text{SiPh}_3$: HL^3) in very good yields and purity. The most salient ^1H NMR spectroscopic feature of these amines is the signal of the NH protons which are found among 4.05 ppm (HL^3), 2.90 (HL^2) and 2.46 ppm (HL^1) as broad singlets. The corresponding lithium salts were obtained by subsequent deprotonation of the amine with *n*-butyl lithium in Et_2O (LiL^3) or *n*-pentane (all other) as white solids in yields of 77% to 96%.

Crystalline LiL^1 ,⁴¹ shows a dimeric structure in the solid state, with a nearly symmetric Li_2N_2 core (Li–N: 1.987(3) Å and Li–N': 2.025(3) Å; Fig. 2, left). The phenyl group of each ligand is oriented towards an adjacent lithium cation (Li–C1: 2.708(3) Å). Furthermore, a Me_{Dipp} group of each ligand is oriented towards a lithium cation with C–Li 2.864(3) Å which is in the range of weak electrostatic interactions (for comparison: agostic Li–H₃C interactions are between 2.0 and 2.2 Å).⁴² LiL^2 and LiL^3 are monomeric in the solid state, with the coordination sphere of lithium

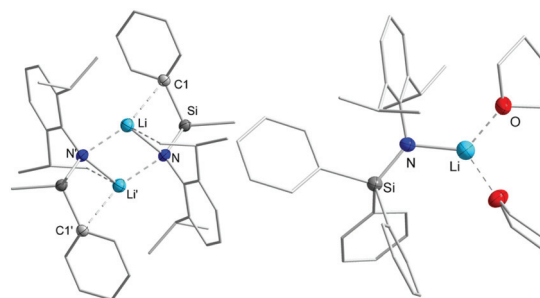


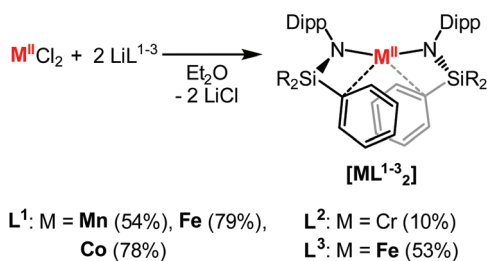
Fig. 2 Crystal structures of the dimeric $(\text{LiN}(\text{Dipp})\text{SiMe}_2\text{Ph})_2$ (LiL^1 , left) from a saturated *n*-pentane solution and the monomeric $\text{LiL}^3 \times (\text{THF})_2$ (LiL^3 , pentane layered saturated THF solution, right). All hydrogen atoms are omitted for clarity.

saturated by THF. Accordingly Li-aryl interactions are absent (Li-C1: 3.772(3) Å (**LiL**²); 3.663(3) Å (**LiL**³)).

Metal complexes bearing a phenyl substituent

The quasilinear metal(II) complexes [**ML**^{*n*}₂] were obtained by reacting one equivalent of the metal chloride (M = Cr-Co) with two equivalents of the respective lithium salt (**LiL**¹-**LiL**³) in diethyl ether. This was comprehensively conducted using **LiL**¹ (M = Cr-Fe), whereas for **LiL**² and **LiL**³ only conceptual reactions were performed with chromium ([**CrL**²₂]) or iron ([**FeL**³₂]) (Scheme 2).

After stirring overnight a colour change of the respective reaction mixtures was observed (Cr: dark green; Mn: beige; Fe: orange/brown; Co: dark red). All volatiles were then removed under reduced pressure, and the solid was redissolved in *n*-pentane to allow separation from the formed lithium chloride. A crystalline material was obtained from saturated *n*-pentane solutions of the compounds at -40 °C in moderate yields. For **L**¹ neutral complexes [**ML**¹₂] (M = Mn-Co) were obtained as crystalline solids in yields of 54% ([**MnL**¹₂]), 79% ([**FeL**¹₂]) and 78% ([**CoL**¹₂]); for chromium only intractable oily substances were observed. This is not particularly surprising, given the reported instability of the related, elusive [Cr(N(Dipp)SiMe₃)₂], for which self-deprotonation and cluster formation were observed.⁴³ Only an increase of the steric profile of the silyl substituents (Si^{*i*}Pr₃ or SiMe^{*t*}Bu₂) gave linear chromium(II) silyl amides.^{21,29} In [**ML**¹₂] (M = Mn-Co) the M-N bond lengths shorten along the series from *ca.* 1.94 Å ([**MnL**¹₂]) to 1.86 Å ([**CoL**¹₂]) (Table 1), which is due to the



Scheme 2 Synthesis of quasilinear metal(II) silylamide complexes [**ML**^{*n*}₂] (**L**¹ = N(Dipp)SiMe₂Ph (M = Mn-Co); **L**² = N(Dipp)SiMePh₂ (M = Cr); **L**³ = N(Dipp)SiPh₃ (M = Fe)).

decrease of ion radii along the series and in agreement with other literature known complexes of the type [M(N(Dipp)SiR₃)₂] (M = Mn-Co).^{7,43-45} The introduced phenyl ring is clearly oriented towards the metal center with M-C₁_{ipso} distances of only 2.800(7) Å for [**MnL**¹₂], 2.696(2) Å for [**FeL**¹₂] and 2.856(2) Å for [**CoL**¹₂]. Consequently, the < N1-M-N2 angles deviate from linearity (compared to [M(N(Dipp)SiMe₃)₂]: 180°) with values of 152.29(17)° (Mn), 150.69(6)° (Fe) and 164.31(7)° (Co) and narrower < M-N-Si bond angles with values of 110.9(2)° (Mn), 108.86(8)° (Fe) and 114.35(8)° (Co) ([M(N(Dipp)SiMe₃)₂]: ≈125°).⁴⁴

For chromium, a comparable complex was obtained employing the more encumbering diphenyl silyl derivative **LiL**² yielding [**CrL**²₂], which was pure by combustion analysis. X-ray analysis on suitable crystals revealed, besides [**CrL**²₂] (see Fig. 3), the presence of co-crystallized (**LiL**²)₂ (17%, see Fig. S84†). In [**CrL**²₂], one of the phenyl rings of one ligand is clearly orientated towards the chromium ion with a Cr-C_{ipso} distance of only 2.372(3) Å. Consequently, the < N1-Cr-N2 bond angle deviates with 140.02° strongly from linearity and the geometry in [**CrL**²₂] is better described as Y-shaped, accounting for the substantial chromium-carbon interaction. The even more sterically demanding triphenylsilyl (**L**³) ligand set was also probed using iron as a representative. [**FeL**³₂] was obtained by reaction of 2 equivalents of **LiL**³ with FeCl₂. In the solid state the closest secondary arene-metal interaction of [**FeL**³₂] is 2.980(2) Å and thus significantly longer than that of [**FeL**¹₂] (2.696(2) Å) (Table 1). The metal-arene interaction M-C2 to the second ligand weakens to a higher extent with a distance of 3.173(2) Å, highlighting the larger steric demand of the **L**³ ligand. Unsurprisingly, the N1-Fe-N2 axis is closer to linearity (162.26(10)°) in comparison to [**FeL**¹₂], whereas the Fe-N slightly shortens to 1.884(2) Å.

The inherent paramagnetism of the samples leads to highly broadened signals in ¹H NMR and prevents any signal assignment for [**MnL**¹₂], as well as [**CrL**²₂] and [**FeL**³₂].^{7,36} In contrast, the proton spectrum of [**CoL**¹₂] is rather well behaved and – together with the one of [Co(N(Dipp)SiMe₃)₂]³⁴ – allowed for a signal assignment. In C₆D₆ the broad signal at 93.4 ppm corresponds to the methyl groups at the silyl moieties of [**CoL**¹₂] (see Fig. S9†). Two contrary shifted signals at 41.6 ppm and -173.2 ppm indicate different electronic environments for the iso-propyl-methyl groups and therefore a hindered rotation

Table 1 Selected bond lengths and angles of compounds [**ML**¹⁻³₂]^{0/-} (**L**¹: M = Mn-Co; **L**²: M = Cr; **L**³: M = Fe) and [**MnL**¹**L**^{1*}]⁻ (* smallest N-Si-C_{Ph} angle)

	Compound	M-N1/M-N2/Å	M-C1/M-C2/Å	N1-M-N2/°	M-N-Si*	N-Si-C _{Ph} *	Torsion angle
Cr	[CrL ² ₂]	1.9515(13)/1.9274(11)	3.318(8)/2.372(3)	140.02(5)	101.75(7)	97.41(11)	39.67(12)
Mn	[MnL ¹ ₂]	1.955(4)/1.941(3)	2.900(4)/2.800(7)	152.29(17)	110.9(2)	100.5(2)	40.0(4)
	[MnL ¹ L ^{1*}] ⁻	2.042(11)/2.160(12)	2.11(2)/3.70(2)	134.4(4)	89.6(5)/134.2(6)	101.4(8)	177.71(10)
Fe	[FeL ¹ ₂]	1.9100(15)/1.9098(15)	2.696(2)/2.8780(18)	150.69(6)	108.86(8)	100.56(8)	40.03(16)
	[FeL ¹ ₂] ⁻	1.905(4)/1.903(4)	3.938(3)/3.859(7)	172.10(17)	116.2(2)	114.4(1)	14.9(5)
	[FeL ³ ₂]	1.889(2)/1.884(2)	2.980(2)/3.173(2)	162.26(10)	112.89(12)	104.01(12)	36.1(2)
	[FeL ³ ₂] ⁻	1.911(3)/1.905(3)	3.605(4)/3.417(3)	172.50(13)	116.64(16)	110.29(15)	45.2(2)
Co	[CoL ¹ ₂]	1.8610(15)/1.8562(15)	2.856(2)/3.2158(17)	164.31(7)	114.35(8)	100.73(7)	37.42(16)
	[CoL ¹ ₂] ⁻	1.883(3)/1.881(3)	3.642(5)/3.707(4)	172.55(13)	113.35(16)	111.34(19)	29.6(4)

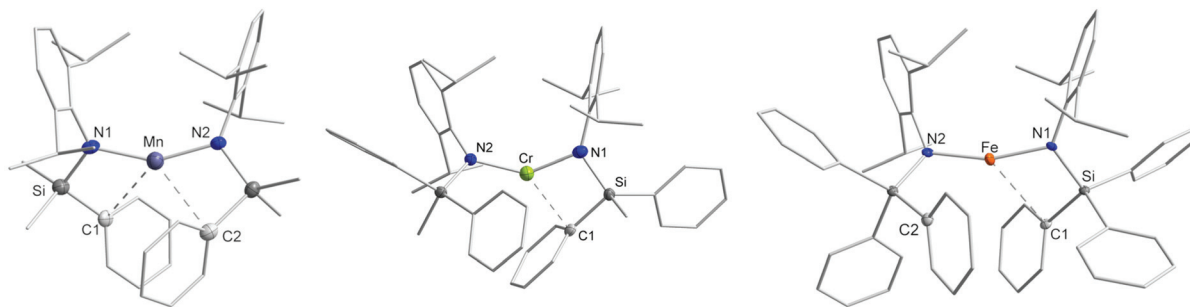
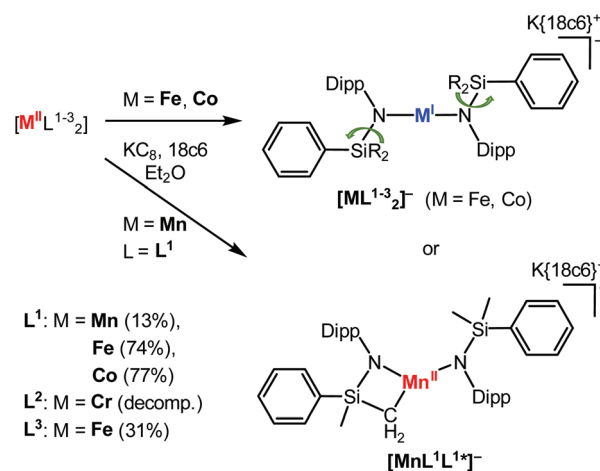


Fig. 3 General structures of $[\text{ML}^{1-3}_2]$ (left: $[\text{ML}^1_2]$ ($\text{M} = \text{Mn-Co}$, depicted for manganese); middle: $[\text{CrL}^2_2]$ (solid solution with dimeric $(\text{LiL}^2)_2$ (17%, not depicted, see also Fig. S84†); right: $[\text{FeL}^3_2]$). All hydrogen atoms are omitted for clarity.

of the ligand sets in solution. The arylc protons of the Dipp moiety cause singlets at 45.6 ppm ($m\text{-CH}_{\text{Dipp}}$) and -45.7 ppm ($p\text{-CH}_{\text{Dipp}}$). The remaining signals at -55.8 ppm and -128.0 ppm can be attributed to the phenyl rings of the silyl fragments. Changing from C_6D_6 to the coordinating THF-d_8 , a broadened signal of the methyl groups at the silyl moieties is now located at 14.2 ppm, whereas the two signals at 24.9 ppm and -30.0 ppm correspond to the methyl groups of the isopropyl groups (see Fig. S10†). While the paramagnetic influence to the protons in *meta*- (41.8 ppm) and *para*- (-31.0 ppm) positions seem to be largely unaffected by the solvent, the three highfield shifted signals at -4.55 ppm, -16.4 ppm and -42.2 ppm indicate a less paramagnetically shifted environment for the phenyl rings. Furthermore, the signal for methine protons, absent in C_6D_6 , is observed at 99.4 ppm. From these observations we tentatively conclude that in coordinating solvents such as THF-d_8 the metal-phenyl interactions are likely replaced by solvent coordination.³⁴ For $[\text{FeL}^1_2]$, similar observations were made, with respect to the solvent dependency (Fig. S7/8†).

Treatment of the metal(II) complexes $[\text{ML}^1_2]$ ($\text{M} = \text{Mn-Co}$) with 1.1 equivalents of potassium graphite in diethyl ether in the presence of one equivalent of 18-crown-6 leads to an immediate colour change of the reaction mixture (Mn: beige \rightarrow dark violet; Fe: orange \rightarrow red; Co: dark red \rightarrow light green). A crystalline material was obtained by diffusion of *n*-pentane into a diethyl ether solution of each compound at -40 °C yielding violet $\text{K}\{18\text{c}6\}[\text{MnL}^1\text{L}^{1*}]^-$, light green $\text{K}\{18\text{c}6\}[\text{FeL}^1_2]^-$, and light green $\text{K}\{18\text{c}6\}[\text{CoL}^1_2]^-$ in yields up to 77% (Scheme 3). Similarly, greenish $\text{K}\{18\text{c}6\}[\text{FeL}^3_2]^-$ was obtained, whereas only decomposition was observed for $[\text{CrL}^2_2]$. X-ray diffraction analysis of $[\text{FeL}^1_2]^-$ and $[\text{CoL}^1_2]^-$ revealed the presence of quasilinear complexes ($[\text{FeL}^1_2]^-$: $172.10(17)^\circ$; $[\text{CoL}^1_2]^-$: $172.55(13)^\circ$) with widening of the $\angle \text{M-N-Si}$ bond angles to values of $116.2(2)^\circ$ ($[\text{FeL}^1_2]^-$) and $113.35(16)^\circ$ ($[\text{CoL}^1_2]^-$) (Fig. 4, middle; Table 1). By losing the metal-arene interaction, the ligands rotate into an eclipsed conformation with torsion angles of $14.9(5)^\circ$ for $[\text{FeL}^1_2]^-$ and $29.6(4)^\circ$ for $[\text{CoL}^1_2]^-$. The M-N bond lengths are mostly unaffected by the reduction of the metal. $[\text{MnL}^1\text{L}^{1*}]^-$ showed intramolecular C-H activation under Mn-C bond formation. A similar behaviour was



Scheme 3 Reduction of $[\text{ML}^{1-3}_2]$ with potassium graphite in the presence of 18-crown-6 lead to the reduced metal(I) complexes $[\text{MnL}^1\text{L}^{1*}]^-$, $[\text{ML}^1_2]^-$ ($\text{M} = \text{Fe, Co}$) and $[\text{FeL}^3_2]^-$.

described for the reaction of CrCl_3 with $\text{LiN}(\text{Dipp})\text{SiMe}_3$ under C-H bond activation of a CH_3 unit of the Dipp moiety.⁴⁶ In the solid state structure of $[\text{MnL}^1\text{L}^{1*}]^-$, whose data set suffers from weakly diffracting crystals, the manganese atom is disordered over two positions (ratio 2 : 1), which is correlated with the bonding to the CH_2 -group of either of the two amide ligands (Fig. 4, left). This leads to a strongly bent N1-Mn-N2 bond axis ($134.4(4)^\circ$) and a distorted trigonal ligand geometry of the resulting manganese(II) ion.

Similar to the compounds comprising the SiMe_2Ph function (L^1), metal-arene interactions are also absent in $[\text{FeL}^3_2]^-$ with its multiple phenyl functions (Fig. 4, right). The N-M-N bond angle is closer to linear ($172.50(13)^\circ$ in $[\text{FeL}^3_2]^-$), with the phenyl rings facing away from the iron center, resulting in a torsion angle of $45.2(2)^\circ$. All other bond lengths and angles in the ligand sets remain the same within standard deviations. This indicates that, even when crowding the metal's sphere with phenyl functions, the metal(I) center in anionic silylamides lacks arene-metal interactions which indicates the absence of significant Lewis-acidity of the 3d-metal(I) ion in linear compounds bearing two anionic ligands.

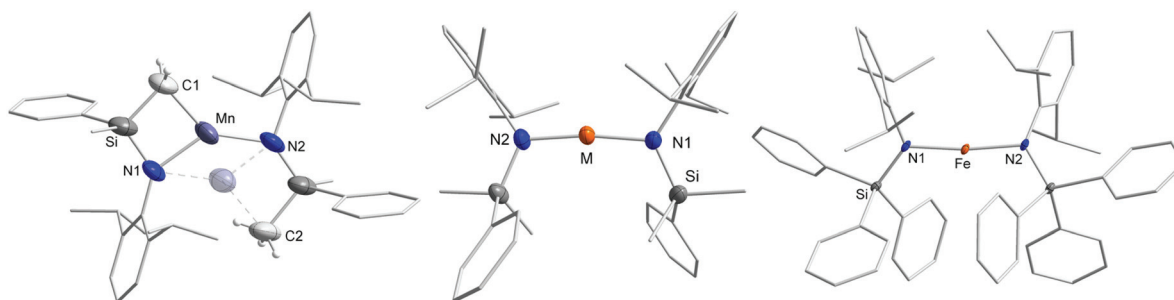


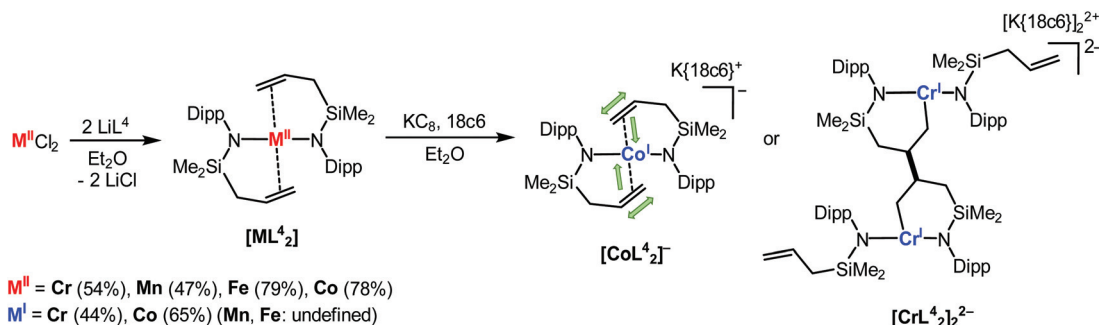
Fig. 4 Sections of the molecular structures of $K\{18c6\}[MnL^1L^{1*}]$ and $K\{18c6\}[ML^n_2]$ in the solid state (left: $[MnL^1L^{1*}]^-$; middle: $[ML^1_2]^-$ ($M = Fe, Co$); right: $[FeL^3_2]^-$). The $K\{18c6\}$ counter ions and hydrogen atoms are generally omitted for clarity. For $[MnL^1L^{1*}]^-$ the disorder of the manganese atom is indicated.

1H NMR spectroscopy also proved expectantly difficult for the monovalent complexes and was only informative for $[CoL^1_2]^-$. By using $[Co(N(Dipp)SiMe_3)_2]^-$ as a reference,^{31,36} the aliphatic signals of the Dipp moiety of $[CoL^1_2]^-$ are found at 17.0/–84.9 ppm ($CH(CH_3)_2$) and at 23.3 ppm ($CH(CH_3)_2$), respectively. Aryl protons in *meta*- and *para*-positions correspond to signals at 14.6 ppm and 2.85 ppm. At 21.4 ppm a broad singlet likely represents the two methyl groups at the silyl moiety, whereas signals at –2.59 ppm, –7.39 ppm and –38.1 ppm belong to protons of the phenyl substituent of the $SiMe_2Ph$ group.

Complexes bearing an allyl substituent

Recently we reported on the distinct interaction of linear anionic metal(i) complexes with alkyne and phosphine substituted alkene substrates.^{32,47} In these cases either the formation of π -complexes or subsequent substrate transformation was observed. As such we wanted to elaborate intramolecular alkene coordination which would also allow for assessing the impact of the oxidation state on the metal–olefin interaction in this coordination geometry. For that we chose $-N(Dipp)SiMe_2(allyl)$ (L^4) as a representative. $LiN(Dipp)SiMe_2(allyl)$ (LiL^4) was obtained in good yields in two steps upon reaction of $ClSiMe_2(allyl)$ with $LiNHDipp$ and subsequent deprotonation of the obtained $HN(Dipp)SiMe_2(allyl)$ (HL^4) with *n*-butyl lithium (see Scheme 1). The most salient 1H NMR spectroscopic feature of HL^4 is the signal for the NH proton at

2.26 ppm measured in C_6D_6 , which is low-field shifted compared to HL^{1-3} (see above). The allyl moiety of HL^4 shows a multiplet from 4.99 to 5.05 ppm for the two terminal alkene protons and a multiplet from 5.81 to 5.95 ppm ($CH=CH_2$), which shifts upon lithiation of the amide to 5.00–5.11 ppm and 6.08–6.25 ppm, respectively. Solid state analysis of LiL^4 could unfortunately not be performed due to the rapid melting of the crystals. Next, two equivalents of LiL^4 were reacted with the respective metal(ii) chloride giving $[ML^4_2]$ ($M = Cr-Co$) in yields of 47%–79% (Scheme 4). In the solid state the amide ligands are arranged in a bent, quasilinear fashion with $\angle N1-M-N2$ angles ranging from 143.61(4) $^\circ$ (Fe) to 150.24(5) $^\circ$ (Cr) (Fig. 5). Both the alkene ligands are situated on the opposing side of the metal with an alkene–M–alkene' angle between 144.3 $^\circ$ ($[MnL^4_2]$) and 148.5 $^\circ$ ($[FeL^4_2]$), the alkene–M–alkene' axis is perpendicular towards the $N1-M-N2$ axis leading to geometries best described as intermediates between the seesaw and tetrahedron ($\tau_4' \approx 0.43-0.47$). The M–N bond lengths shorten from Cr (2.0129(13) Å) to Co (1.9262(7) Å) (see Table 2), but are overall longer than those in $[ML^1_2]$, probably due to the higher coordination number. M–alkene distances amount to 2.3243(4) Å (Cr), 2.6475(4) Å (Mn), 2.4351(3) Å (Fe) and 2.4437(3) Å (Co), with C=C bond lengths of 1.330(3) Å (Mn) or around 1.34 Å (Cr: 1.346(2) Å, Fe: 1.3418(17) Å, and Co: 1.3421(13) Å), respectively. Structural examples of metal(ii)–alkene interactions are absent for manganese and generally scarce for other 3d metals. In these,



Scheme 4 Synthesis of $[ML^4_2]$ ($M = Cr-Co$) and stepwise reduction to $[CoL^4_2]^-$ and $[CrL^4_2]^{2-}$.

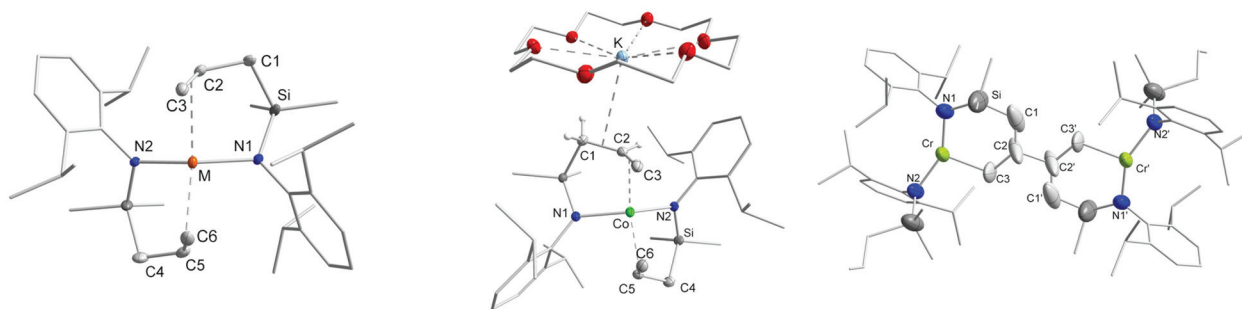


Fig. 5 Molecular structures of $[\text{ML}^4_2]$ ($\text{M} = \text{Cr-Co}$; left), $[\text{CoL}^4_2]^-$ (middle) and the anionic section of $[\text{CrL}^4_2]_2^{2-}$ (right). Non-coordinating $\text{K}(18\text{c}6)$ moieties and unnecessary hydrogen atoms are omitted for clarity.

Table 2 Selected structural values of the neutral $[\text{ML}^4_2]$ ($\text{M} = \text{Cr-Co}$) and the reduced species $[\text{CoL}^4_2]^-$

	Compound	M-N1/M-N2/Å	C2=C3/C5=C6	M ^{III} -C=C	N1-M-N2/°	CC-M-CC/°
Cr	$[\text{CrL}^4_2]$	2.0155(12)/2.0129(13)	1.346(2)/1.348 (2)	2.3243(4)/2.3457(3)	150.24(5)	147.33(1)
Mn	$[\text{MnL}^4_2]$	2.0040(15)/2.0030(15)	1.330(3)/1.337(3)	2.6618(3)/2.6475(4)	149.26(6)	144.30(1)
Fe	$[\text{FeL}^4_2]$	1.9546(9)/1.9544(9)	1.3418(17)/1.343(2)	2.4824(3)/2.4351(3)	143.61(4)	148.59(1)
Co	$[\text{CoL}^4_2]$	1.9262(7)/1.9280(7)	1.3421(13)/1.3444(16)	2.4653(3)/2.4437(3)	144.37(3)	144.49(1)
	$[\text{CoL}^4_2]^-$	2.0142(14)/2.0248(14)	1.379(3)/1.369(3)	2.0337(3)/2.0646(4)	138.08(6)	138.53(1)

longer C=C bond distances are found for chromium (1.43 Å),⁴⁸ iron (1.36–1.41 Å)^{49–53} and cobalt (1.37–1.38 Å)^{54,55} complexes with closer distances between the metal and the alkene (Cr: 2.13 Å;⁴⁸ Fe: 1.93–2.23 Å;^{49–53} Co: 1.94–1.95 Å (ref. 54 and 55)). The observed C=C lengths in $[\text{ML}^4_2]$ are close to non-coordinating allylsilyl units⁵⁶ and cationic magnesium (II)- π -alkene compounds, in which backbonding is absent (C=C: 1.32–1.35 Å).⁵⁷ From this we conclude that the metal-alkene interactions in $[\text{ML}^4_2]$ are weak and mostly electrostatic. Similar to $[\text{ML}^{1-3}]$, the evaluation of $[\text{ML}^4_2]$ *via* ¹H NMR spectroscopy was only partially possible due to the compound's paramagnetism. Best results were again received for cobalt ($[\text{CoL}^4_2]$), with similarities to the signal distribution of $[\text{CoL}^1_2]$ (compare Fig. S33 and 34†)

In C₆D₆ the methyl groups of the silyl fragment experience smaller paramagnetic shifting effects with a signal at 26.5 ppm. Additionally, the allylic chain in $[\text{CoL}^4_2]$ evokes broad signals at 57.1 ppm, –48.0 ppm and –164 ppm. Interestingly, no remarkable changes in the shifts are observable by measuring $[\text{CoL}^4_2]$ in THF-d₈, indicating persistent coordination of the alkene unit to the cobalt ion, or by preventing THF coordination.

Reduction of $[\text{ML}^4_2]$ ($\text{M} = \text{Cr-Co}$) with 1.1 equivalents of potassium graphite in diethyl ether in the presence of one equivalent of 18-crown-6 was subsequently conducted. For manganese and iron only the formation of lightly coloured, unidentifiable solids, which led to decomposition, were obtained. For cobalt, the envisioned silylamide complex $[\text{CoL}^4_2]^-$ could be obtained in 65% yield, whose structure was verified by X-ray diffraction analysis. In comparison to the divalent $[\text{CoL}^4_2]$, the interaction between the metal ion and the allyl unit is stronger, with a shorter Co-alkene distance of 2.0337(3) Å in $[\text{CoL}^4_2]^-$ (–0.4 Å *vs.* $[\text{CoL}^4_2]$) as well as elonga-

tion of the C=C bond to 1.379(3) Å (+0.035 Å *vs.* $[\text{CoL}^4_2]$). The C=C bond activation is slightly lower than that found for other low-valent, low-coordinate cobalt-alkene complexes (1.39–1.44 Å),^{54,58} which speaks to only moderate π -backbonding in $[\text{CoL}^4_2]^-$. In comparison to the parent $[\text{Co}(\text{N}(\text{Dipp})\text{SiMe}_3)_2]^-$, the ¹H NMR signals of the alkene unit in $[\text{CoL}^4_2]^-$ are found at 47.4 ppm, 23.4 ppm and 9.71 ppm, which indicates coordinative interactions also in solution. For chromium, a green compound was isolated, whose combustion data were in agreement with $[\text{CrL}^4_2]^-$. However, X-ray diffraction analysis revealed the presence of a dimeric compound in which two $[\text{CrL}^4_2]$ units are connected *via* a C–C bond in the β -position of an allyl substituent. Although the structure suffered from intrinsic crystallographic flaws, due to weakly diffracting crystals, tentative examination of the bond lengths shows the presence of a C–C single bond of the former C=C bond unit as well as a clear presence of a Cr–C bond. The second allyl ligand of each complex part is pointing away from the respective metal ion, which contrasts the observations for $[\text{CoL}^4_2]^-$. This gives a T-shaped coordination geometry around each chromium ion. We rationalize the formation of $[\text{CrL}^4_2]_2^{2-}$ as follows: first, reduction of $[\text{CrL}^4_2]$ leads to the envisioned monovalent chromium complex “ $[\text{CrL}^4_2]^-$ ” with internal π -alkene coordination. This can alternatively be described as a chromium(II) ion bound to an alkene radical anion, similar to the observations made by us and others for related metal alkyne complexes.^{47,59} These radical anions would undergo subsequent intermolecular C–C coupling which gives the dimeric complex $[\text{CrL}^4_2]_2^{2-}$. The behaviour of the bound alkene unit overall resembles the electrochemical reductive dimerisation of activated alkenes.⁶⁰ $[\text{CrL}^4_2]_2^{2-}$ exhibits a magnetic moment of 6.17 μ_B which speaks to weakly antiferromagnetically coupled high-spin chromium(II) ions.

Magnetic properties of $[\text{ML}^n_2]^{-0}$ complexes in solution

Having understood the different behaviours of the functional groups (Ph vs. allyl) in solution, we were interested in how the secondary ligand coordination impacts the magnetic properties of $[\text{ML}^{1-4}_2]$ in solution which we probed with the Evans method (Table 3). The μ_{eff} of $5.65\mu_{\text{B}}$ for $[\text{MnL}^1_2]$ is close to the spin-only value of $5.92\mu_{\text{B}}$ and similar to $[\text{Mn}(\text{N}(\text{Dipp})\text{SiMe}_3)_2]$ ($6.09\mu_{\text{B}}$).⁷

$[\text{FeL}^1_2]$ and $[\text{CoL}^1_2]$ exhibit expectantly higher than spin-only values due to orbital contributions. For $[\text{CrL}^2_2]$ the effective magnetic moment of $\mu_{\text{eff}} = 3.24\mu_{\text{B}}$ is substantially lower than the spin-only value of $4.89\mu_{\text{B}}$ (quintet state (d^4)) and in stark contrast to comparable complexes like $[\text{Cr}^{\text{II}}(\text{N}(\text{Dipp})\text{Si}^i\text{Pr}_3)_2]$ ($\mu_{\text{eff}} = 4.9\mu_{\text{B}}$).²⁹ Unquenched negative orbital contributions are to be expected for a d^4 system, however, the extent in the case of $[\text{CrL}^2_2]$ indicates further unresolved differences in the electronic structure. The magnetic moment of $[\text{FeL}^3_2]$ of $4.88\mu_{\text{B}}$ equals the spin-only value ($\mu_{\text{S.O.}} = 4.89$) without any further orbital contributions. Similarly, a high-spin character was found for all $[\text{ML}^4_2]$ complexes. For $[\text{CrL}^4_2]$, μ_{eff} amounted to $4.45\mu_{\text{B}}$, which is slightly less than the spin-only value of $4.89\mu_{\text{B}}$ ($S = 2$). For $[\text{MnL}^4_2]$, the μ_{eff} value ($5.27\mu_{\text{B}}$) is also lower than the expected $\mu_{\text{S.O.}}$ value ($5.92\mu_{\text{B}}$, $S = 5/2$). In contrast, for iron ($5.14\mu_{\text{B}}$; $\mu_{\text{S.O.}} = 4.89\mu_{\text{B}}$) and especially cobalt ($4.84\mu_{\text{B}}$; $\mu_{\text{S.O.}} = 3.87\mu_{\text{B}}$), values higher than the spin-only values are again obtained. This is in general agreement with other linear metal(II) complexes. Diminished contributions from orbital angular momentum are generally observed which is expected due to deviations from linearity and additional coordinative interactions.^{4,9,12,20,22-24} With an effective magnetic moment of $5.37\mu_{\text{B}}$ ($\mu_{\text{S.O.}} = 5.92\mu_{\text{B}}$), $[\text{MnL}^1\text{L}^{1*}]^-$ is a high-spin metal(II) complex with five unpaired electrons. $[\text{FeL}^{1/3}_2]^-$ and $[\text{CoL}^1_2]^-$ retain their higher than spin-only values with $\mu_{\text{eff}} = 4.52\mu_{\text{B}}/4.60\mu_{\text{B}}$ ($\mu_{\text{S.O.}} = 3.87\mu_{\text{B}}$) and $\mu_{\text{eff}} = 3.94\mu_{\text{B}}$ ($\mu_{\text{S.O.}} = 2.83\mu_{\text{B}}$), respectively. Those values resemble the ones for $[\text{M}(\text{N}(\text{Dipp})\text{SiMe}_3)_2]^-$ ($\text{M} = \text{Fe}$ ($\mu_{\text{eff}} =$

$4.34\mu_{\text{B}}$); Co ($\mu_{\text{eff}} = 3.93\mu_{\text{B}}$)³⁶ is to be expected given the proposed absence of any metal-aryl interactions. The magnetic susceptibility of $[\text{CoL}^4_2]^-$ ($\mu_{\text{eff}} = 4.04\mu_{\text{B}}$) is comparable to that of $[\text{CoL}^1_2]^-$ indicating that here the additional allyl coordination does not negatively impact the orbital contributions to the magnetic moment. However, pronounced contributions from a description of $[\text{CoL}^4_2]^-$ as a cobalt(II) bound alkene radical anion, mimicking π -alkyne adducts of linear metal(I) silylamides,⁴⁷ are also possible.

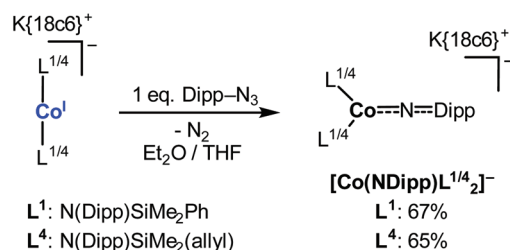
Imido cobalt complexes

As recently shown, linear cobalt(I) silylamides are valuable platforms for the generation of unique imido cobalt complexes in higher spin states.^{37,38} Those studies also showed that these imido cobalt units do not interact with alkenes (*e.g.* under C=C bond aziridation) or other electron rich substrates (phosphines). In contrast, it is highly competent in H atom abstraction from external C-H bonds.³⁸ To elaborate further on the suitability of linear cobalt(I) complexes to support an [NR] unit in higher spin states, we conducted respective studies using $[\text{CoL}^1_2]^-$ and $[\text{CoL}^4_2]^-$ as examples. The latter was of special interest due to possible intramolecular aziridation. $[\text{CoL}^1_2]^-$ and $[\text{CoL}^4_2]^-$ were reacted with one equivalent of Dipp-N₃, respectively, which was recently used to yield unique cobalt imidyl radical complexes using the parent silylamide complex $\text{K}\{\text{m}\}[\text{Co}(\text{N}(\text{Dipp})\text{SiMe}_3)_2]^-$ ($\text{m} = \text{none}, 18\text{c}6, \text{crypt}$).³⁸ The corresponding reactions in a 1:1 (v/v) mixture of THF/Et₂O gave dark green $[\text{Co}(\text{NDipp})\text{L}^1_2]^-$ and dark red $[\text{Co}(\text{NDipp})\text{L}^4_2]^-$ in yields of 67% and 65%, respectively (Scheme 5).

In both compounds (Fig. 6), the cobalt ions exhibit a trigonal planar coordination motif with two amide and one NDipp ligands. For $[\text{Co}(\text{NDipp})\text{L}^1_2]^-$, the Co-N_{imido} bond length amounts to 1.7707(17) Å with a symmetry generated linear Co-N-Dipp axis (180°). For $[\text{Co}(\text{NDipp})\text{L}^4_2]^-$ the situation is similar (Co-N_{imido} 1.7555(16) Å, Co-N-Dipp 176.95(16)°). The observed cobalt imide bond lengths are remarkable, as they are usually found between 1.61 and 1.70 Å.⁶³ They slightly surpasses even those of the recently reported $\text{K}\{18\text{c}6\}[\text{Co}(\text{NDipp})\text{N}(\text{Dipp})\text{SiMe}_3)_2]$ (Co-N 1.751(2)), a unique high-spin system with substantial imidyl radical character on the imide nitrogen.³⁷ For $[\text{Co}(\text{NDipp})\text{L}^1_2]^-$ and $[\text{Co}(\text{NDipp})\text{L}^4_2]^-$ magnetic moments of $4.87\mu_{\text{B}}$ and $5.05\mu_{\text{B}}$ are observed, indicating a quintet state. As such the obtained imido complexes are tenta-

Table 3 Magnetic susceptibilities in solution using the Evans method (C₆D₆ for neutral, THF-d₈ for anionic complexes)^{61,62}

	Compound	μ_{eff} [μ_{B}] ($\mu_{\text{S.O.}}$ [μ_{B}])
Cr	$[\text{CrL}^2_2]$	3.24 (4.89)
	$[\text{CrL}^4_2]$	4.45 (4.89)
	$[\text{CrL}^4_2]_2^{2-}$	6.17 (6.93)
Mn	$[\text{MnL}^1_2]$	5.65 (5.92)
	$[\text{MnL}^1\text{L}^{1*}]^-$	5.37 (5.92)
Fe	$[\text{MnL}^4_2]$	5.27 (5.92)
	$[\text{FeL}^1_2]$	5.23 (4.89)
	$[\text{FeL}^1_2]^-$	4.52 (3.87)
	$[\text{FeL}^3_2]$	4.88 (4.89)
	$[\text{FeL}^3_2]^-$	4.60 (3.87)
	$[\text{FeL}^4_2]$	5.14 (4.89)
Co	$[\text{CoL}^1_2]$	4.89 (3.87)
	$[\text{CoL}^1_2]^-$	3.94 (2.83)
	$[\text{CoL}^4_2]$	4.84 (3.87)
	$[\text{CoL}^4_2]^-$	4.04 (2.83)
	$[\text{Co}(\text{NDipp})\text{L}^1_2]^-$	4.87 (4.89)
	$[\text{Co}(\text{NDipp})\text{L}^4_2]^-$	5.05 (4.89)



Scheme 5 Reactivity of $[\text{CoL}^{1/4}_2]^-$ towards Dipp-N₃ resulting in the imido complexes $[\text{Co}(\text{NDipp})\text{L}^{1/4}_2]^-$.

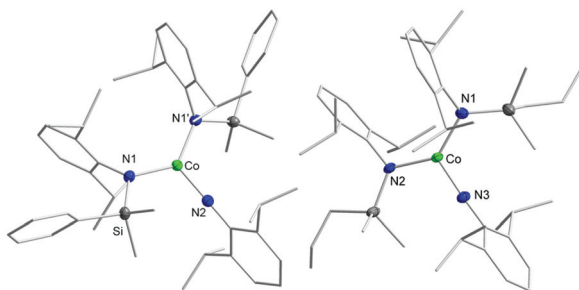


Fig. 6 Sections of the crystal structures $[\text{Co}(\text{NDipp})\text{L}^4_2]^-$ (left) and $[\text{Co}(\text{NDipp})\text{L}^4_2]^-$ (right). Cations and H atoms are omitted for clarity. $[\text{Co}(\text{NDipp})\text{L}^4_2]^-$: Co–N2 1.7707(17) Å, Co–N1/N1' 1.9493(12) Å, N1–Co–N1' 128.17(7)°, Co–N2–C 180.0°; $[\text{Co}(\text{NDipp})\text{L}^4_2]^-$: Co–N3 1.7555(16) Å, Co–N1 1.9378(18) Å, Co–N2 1.9230(18) Å, N1–Co–N1' 134.35(7)°, Co–N3–C 176.95(16)°.

tively described as very rare examples of high-spin imido cobalt species.^{37,64} The case of $[\text{Co}(\text{NDipp})\text{L}^4_2]^-$ is especially remarkable as it exhibits an alkene function in the vicinity of the $[\text{MNR}]$ unit. Generally, late 3d-metal imido complexes are potent in the aziridation of alkene substrates,⁶⁵ which is not observed here, even after prolonged storage at ambient temperature, heating to 50 °C or light irradiation (400 nm). Steric constraints or a pronounced nucleophilic character of the imidyl radical, which mitigates its aziridation reactivity, might be the reason for this.

Conclusion

We reported the synthesis of quasilinear homoleptic metal(II) complexes $[\text{M}(\text{N}(\text{Dipp})\text{SiMe}_n\text{Ph}_{3-n})_2]$ of Cr–Co. The presence of phenyl substituents gives rise to secondary metal–arene interactions, reflected by a bent N–M–N axis. Reduction of these compounds with KC_8 in the presence of 18-crown-6 gave the corresponding metal(I) complexes for iron and cobalt, where metal–arene interactions are absent. These findings show, at the structural level, that in anionic quasilinear metal complexes the metal(I) ion exhibits negligible Lewis acidity, contrasting the situation in the divalent, neutral counterparts. For manganese, C–H bond activation of a SiMe_3 -unit is observed. The introduction of a propenyl substituent into the ligand set (using $-\text{N}(\text{Dipp})\text{SiMe}_2(\text{allyl})$) gave divalent complexes with intramolecular alkene coordination, a feature not reported so far for divalent manganese. The propenyl–metal interaction is rather weak which is indicated by long M–alkene and C=C bond lengths. For cobalt, reduction leads to enhanced π -backbonding and for chromium even to an intermolecular reductive C–C coupling of the propene unit upon formation of a binuclear chromium(II) alkyl complex. These results emphasize the intricacies of metal–bond interactions in the case of low-valent and low-coordinate metal ions, and reveal that in anionic linear metal(I) complexes, the metal ion should not be regarded as coordinatively and electronically deficient, but rather electron rich. The obtained cobalt complexes were

further reacted with an aryl azide, resulting in rare examples of high-spin imido cobalt complexes. This is remarkable in the case of propenyl substituted ancillary ligands, as the alkene function does not react with the imido metal unit, an usually observed behaviour for imido metal units. The aptitude of silylamides in the stabilization of imido metal units in higher spin states as well as the potential to introduce (coordinatively labile) functionalities in the vicinity of a quasi-two-coordinate metal ion is currently developed in our lab.

Experimental section

Materials and methods

All manipulations were carried out in a glovebox under a dry argon atmosphere, unless indicated otherwise. Used solvents were dried by continuous distillation over sodium metal for several days, degassed *via* three freeze–pump–thaw cycles and stored over molecular sieves 4 Å. Deuterated solvents were used as received, degassed *via* three freeze–pump cycles and stored over molecular sieves 4 Å. The ^1H NMR spectra were recorded on a Bruker AV 500, a Bruker HD 500 or a Bruker HD 300 NMR spectrometer (Bruker Corporation, Billerica, USA). Chemical shifts are reported in ppm relative to the residual proton signals of the solvent (for ^1H). $w_{1/2}$ is the line width of a signal at half its maximum intensity. Integrals of the broad signals of the ligand set were obtained directly or by peak fitting (in the case of overlapping signals) using the MestreNova software package (Mestrelab, Santiago de Compostela, Spain). Solution magnetic susceptibility was determined using the Evans method from at least two independent samples.^{61,62} IR measurements were conducted on a Bruker Alpha ATR-IR spectrometer (Bruker Corporation, Billerica, USA). The UV/VIS measurement was recorded on an AnalytikJena Specord S600 using the WinASPECT software. Elemental analysis was performed by the “in-house” service of the Chemistry Department of Philipps University Marburg, Germany, using a CHN(S) analyser vario MICRO cube (Elementar Analysensysteme GmbH, Langenselbold, Germany).

$-\text{N}(\text{Dipp})\text{SiMe}_2\text{Ph}$ (L^1) containing compounds

HL¹. The compound is known in the literature, but so far not isolated and used without analysis.^{39,41} 5.62 mL of 2,6-diisopropylaniline (30 mmol, 1 equiv.) were cooled to -20 °C in Et_2O before adding 1 equivalent of *n*-BuLi (30 mmol, 1 equiv.) dropwise. The mixture was stirred at room temperature for one hour before it was cooled to -20 °C, again. A precooled solution of 5.00 mL of chloro(dimethyl)phenyl silane (30 mmol, 1 equiv.) in Et_2O was added slowly, whereas a light yellow solution and a colourless precipitate appeared. The reaction mixture was allowed to stir overnight at room temperature before the solvent was removed *in vacuo*. After condensation of the remaining residue (120 °C, 10^{-3} mbar), the desired product (**HL¹**) was obtained as a colourless, viscous liquid in a yield of 97%. **Yield:** 9.10 g (29 mmol, 97%). **^1H NMR:**

(300.2 MHz, C₆D₆, 300 K, ppm): δ = 7.54–7.57 (m, 2 H, ArH), 7.19–7.26 (m, 3 H, ArH), 7.04–7.11 (m, 3 H, ArH), 3.40 (h, 2 H, ³J_{H,H} = 6.82 Hz, CH(CH₃)₂), 2.46 (bs, 1 H, NH), 1.12 (d, 12 H, ³J_{H,H} = 6.84 Hz, CH(CH₃)₂), 0.32 (s, 6 H, Si(CH₃)₂). ¹³C-{¹H} NMR: (75.5 MHz, C₆D₆, 300 K, ppm): δ = 144.2 (s, NC_{ipso}), 140.0 (s, *o*-C_{Dipp}), 139.5 (s, SiC_{ipso}), 133.6 (s, *o*-CH_{Ph}), 129.5 (s, *p*-CH_{Ph}), 128.1 (*m*-CH_{Ph}), 124.2 (s, *p*-CH_{Dipp}), 123.4 (s, *m*-CH_{Dipp}), 28.6 (s, CH(CH₃)₂), 23.8 (s, CH(CH₃)₂), -0.70 (s, Si(CH₃)₂).

LiL¹. The compound is known in the literature, but so far not isolated and used without analysis.⁴¹ 6.50 g (20.8 mmol, 1 equiv.) of **HL¹** were dissolved in 20 mL of *n*-pentane. It was cooled to -20 °C and *n*-BuLi (20.8 mmol, 1 equiv.) was added dropwise, while a white precipitate appeared immediately. After stirring for a further 30 minutes, the solid was filtered off and washed with *n*-pentane before drying *in vacuo*. **LiL¹** could be obtained as a white solid in a yield of 77%. **Yield:** 5.06 g (16.0 mmol, 77%). Crystals, suitable for X-ray diffraction analysis, were obtained from a saturated *n*-pentane solution of **LiL¹** at -40 °C. ¹H NMR: (300.2 MHz, C₆D₆, 300 K, ppm): δ = 7.81–7.83 (m, 2 H, *m*-CH_{Dipp}), 7.32–7.37 (m, 2 H, *m*-CH_{Ph}), 7.21–7.26 (m, 1 H, *p*-CH_{Dipp}), 6.81–6.93 (m, 3 H, *o/p*-CH_{Ph}), 3.07 (h, 2 H, ³J_{H,H} = 6.83 Hz, CH(CH₃)₂), 1.16 (d, 6 H, ³J_{H,H} = 6.67 Hz, CH(CH₃)₂), 0.52 (d, 6 H, ³J_{H,H} = 7.01 Hz, CH(CH₃)₂), 0.30 (s, 6 H, Si(CH₃)₂). ¹³C-{¹H} NMR: (300.2 MHz, C₆D₆, 300 K, ppm): δ = 149.3 (s, NC_{ipso}), 143.1 (s, *o*-C_{Dipp}), 142.9 (s, SiC_{ipso}), 133.4 (s, *o*-CH_{Ph}), 129.9 (m, *m/p*-CH_{Ph}), 124.3 (s, *m*-CH_{Dipp}), 120.3 (s, *p*-CH_{Dipp}), 27.7 (s, CH(CH₃)₂), 25.3 (s, CH(CH₃)₂), 24.7 (s, CH(CH₃)₂), 0.98 (s, Si(CH₃)₂). ¹H NMR: (300.2 MHz, THF-d₈, 300 K, ppm): δ = 7.54–7.57 (m, 2 H, *m*-CH_{Ph}), 7.05–7.16 (m, 3 H, *o/p*-CH_{Ph}), 6.73 (d, 2 H, ³J_{H,H} = 7.45 Hz, *m*-CH_{Dipp}), 6.37 (d, 1 H, ³J_{H,H} = 7.41 Hz, *p*-CH_{Dipp}), 4.05 (h, ³J_{H,H} = 6.90 Hz, 2 H, CH(CH₃)₂), 0.99 (d, 12 H, ³J_{H,H} = 6.93 Hz, CH(CH₃)₂), 0.17 (s, 6 H, Si(CH₃)₂). ¹³C-{¹H} NMR: (75.5 MHz, THF-d₈, 300 K, ppm): δ = 157.4 (s, NC_{ipso}), 149.2 (s, SiC_{ipso}), 143.8 (s, *o*-C_{Dipp}), 134.5 (s, *o*-CH_{Ph}), 127.4 (s, *m*-CH_{Ph}), 127.2 (s, *p*-CH_{Ph}), 122.5 (s, *m*-CH_{Dipp}), 115.4 (s, *p*-CH_{Dipp}), 27.2 (s, CH(CH₃)₂), 25.3* (s, CH(CH₃)₂), 2.96 (s, Si(CH₃)₂). *, The signal partially overlaps with the solvent signal. Elemental analysis of C₂₀H₂₈LiNSi (317.48 g mol⁻¹): calcd: N 4.41, C 75.67, H 8.89; found: N 4.91, C 76.11, H 8.89%. **IR** (ATR, cm⁻¹): $\tilde{\nu}$ = 3068 (w), 3043 (w), 3007 (w), 2958 (m), 2922 (w), 2903 (w), 2866 (m), 1586 (w), 1458 (w), 1418 (s), 1387 (w), 1363 (w), 1308 (m), 1231 (s), 1188 (s), 1143 (w), 1104 (m), 1050 (w), 1040 (m), 997 (w), 921 (vs), 882 (m), 824 (m), 813 (m), 798 (m), 775 (vs), 755 (vs), 737 (s), 701 (s), 668 (m), 619 (w), 593 (w), 572 (m), 531 (m), 478 (m), 451 (w), 436 (m), 413 (m).

[ML¹]₂ (M = Mn–Co). One equivalent of MCl₂ (M = Mn–Co) and two equivalents of **LiL¹** were suspended in 15 mL of diethyl ether. It was allowed to stir overnight at room temperature, while a change in colour was observed (Mn: beige → dark beige; Fe: yellow → orange-brown; Co: light yellow → dark red-brown). All volatiles were removed under reduced pressure before resolving the obtained residue in *n*-pentane. The lithium chloride was filtered off and it was cooled to -40 °C for crystallization. After several days the solution was decanted

off. Crystalline **[ML¹]₂** (M = Mn–Co) was obtained in yields of 54–79%.

[MnL¹]₂. Using 79 mg of MnCl₂ (0.63 mmol, 1 equiv.), **[MnL¹]₂** could be obtained as a yellow-orange crystalline solid. **Yield:** 230 mg (0.34 mmol, 54%). Crystals, suitable for X-ray diffraction analysis, were obtained from a saturated *n*-pentane solution of **[MnL¹]₂** at -40 °C. Elemental analysis of C₄₀H₅₆MnN₂Si₂ (676.01 g mol⁻¹): calcd: N 4.14, C 71.07, H 8.35; found: N 4.56, C 70.67, H 8.27%. **IR** (ATR, cm⁻¹): $\tilde{\nu}$ = 3068 (w), 3050 (w), 3015 (w), 2954 (s), 2924 (m), 2865 (m), 1588 (w), 1563 (w), 1482 (w), 1457 (m), 1425 (s), 1400 (w), 1380 (m), 1360 (m), 1310 (s), 1239 (s), 1195 (s), 1159 (w), 1145 (w), 1104 (s), 1049 (w), 1039 (m), 997 (w), 972 (w), 924 (s), 879 (w), 834 (s), 795 (m), 779 (vs), 766 (vs), 733 (s), 714 (w), 704 (s), 692 (s), 672 (m), 644 (w), 621 (w), 592 (m), 536 (m), 503 (w), 466 (m), 441 (m), 426 (s). **Evans** (500.1 MHz, 300 K, C₆D₆ + 1% TMS): μ_{eff} = 5.65 μ_{B} ; $\mu_{\text{s.o.}}$ = 5.92 μ_{B} .

[FeL¹]₂. Using 60 mg of FeCl₂ (0.47 mmol, 1 equiv.), **[FeL¹]₂** could be obtained as a yellow-orange crystalline solid. **Yield:** 250 mg (0.37 mmol, 79%). Crystals, suitable for X-ray diffraction analysis, were obtained from a saturated *n*-pentane solution of **[FeL¹]₂** at -40 °C. ¹H NMR (300.2 MHz, C₆D₆, 300 K, ppm): δ = 98.0 (bs, 12 H, $w_{\frac{1}{2}}$ = 1870 Hz, Si(CH₃)₂), 40.8 (bs, 4 H, $w_{\frac{1}{2}}$ = 450 Hz, *m*-CH_{Dipp}), 29.6 (bs, 14 H, $w_{\frac{1}{2}}$ = 580 Hz, CH(CH₃)₂), -32.0 (bs, $w_{\frac{1}{2}}$ = 222 Hz, CH_{Ph}), -50.3 (bs, 2 H, $w_{\frac{1}{2}}$ = 266 Hz, *p*-CH_{Dipp}), -61.3 (bs, 4 H, $w_{\frac{1}{2}}$ = 460 Hz, CH_{Ph}), -108 (bs, 4 H, $w_{\frac{1}{2}}$ = 2000 Hz, CH_{Ph}), -136.9 (bs, 12 H, $w_{\frac{1}{2}}$ = 2470 Hz, CH(CH₃)₂). ¹H NMR (300.2 MHz, THF-d₈, 300 K, ppm): δ = 61.4 (s, 4 H, $w_{\frac{1}{2}}$ = 150 Hz, *m*-CH_{Dipp}), 38.6 (bs, 4 H, $w_{\frac{1}{2}}$ = 2140 Hz, CH(CH₃)₂), 23.7 (s, 12 H, $w_{\frac{1}{2}}$ = 160 Hz, CH(CH₃)₂), 13.8 (bs, 12 H, $w_{\frac{1}{2}}$ = 565 Hz, Si(CH₃)₂), -3.53 (bs, $w_{\frac{1}{2}}$ = 48 Hz, CH_{Ph}), -8.73 (s, $w_{\frac{1}{2}}$ = 86 Hz, CH_{Ph}), -26.0 (bs, $w_{\frac{1}{2}}$ = 74 Hz, *p*-CH_{Dipp}), -26.3 (bs, $w_{\frac{1}{2}}$ = 1020 Hz, CH_{Ph}), -64.1 (bs, 12 H, $w_{\frac{1}{2}}$ = 690 Hz, CH(CH₃)₂). Elemental analysis of C₄₀H₅₆FeN₂Si₂ (676.92 g mol⁻¹): calcd: N 4.14, C 70.97, H 8.34; found: N 4.43, C 70.60, H 8.24%. **IR** (ATR, cm⁻¹): $\tilde{\nu}$ = 3050 (w), 3016 (w), 2954 (m), 2925 (m), 2865 (m), 1588 (w), 1563 (w), 1482 (w), 1457 (m), 1425 (s), 1401 (w), 1381 (m), 1360 (m), 1332 (w), 1310 (s), 1239 (s), 1193 (s), 1159 (w), 1146 (w), 1105 (s), 1050 (w), 1039 (m), 996 (w), 956 (w), 918 (s), 879 (w), 839 (s), 782 (vs), 767 (vs), 733 (s), 715 (m), 701 (s), 674 (m), 595 (m), 535 (m), 464 (m), 442 (m), 426 (s). **Evans** (500.1 MHz, 300 K, C₆D₆ + 1% TMS): μ_{eff} = 5.20 μ_{B} ; $\mu_{\text{s.o.}}$ = 4.89 μ_{B} .

[CoL¹]₂. Using 82 mg of CoCl₂ (0.63 mmol, 1 equiv.), **[CoL¹]₂** could be obtained as a dark red crystalline solid. **Yield:** 333 mg (0.49 mmol, 78%). Crystals, suitable for X-ray diffraction analysis, were obtained from a saturated *n*-pentane solution of **[CoL¹]₂** at -40 °C. ¹H NMR (300.2 MHz, C₆D₆, 300 K, ppm): δ = 93.4 (bs, 12 H, $w_{\frac{1}{2}}$ = 1330 Hz, Si(CH₃)₂), 45.6 (bs, 4 H, $w_{\frac{1}{2}}$ = 358 Hz, *m*-CH_{Dipp}), 41.6 (bs, 12 H, $w_{\frac{1}{2}}$ = 345 Hz, CH(CH₃)₂), -45.7 (bs, 2 H, $w_{\frac{1}{2}}$ = 271 Hz, *p*-CH_{Dipp}), -55.8 (bs, 8 H, $w_{\frac{1}{2}}$ = 326 Hz, CH_{Ph}), -128.0 (bs, 2 H, $w_{\frac{1}{2}}$ = 1560 Hz, CH_{Ph}), -173.2 (bs, 12 H, $w_{\frac{1}{2}}$ = 1780 Hz, CH(CH₃)₂). ¹H NMR (300.2 MHz, THF-d₈, 300 K, ppm): δ = 99.4 (s, 4 H, $w_{\frac{1}{2}}$ = 1080 Hz, CH(CH₃)₂), 41.8 (s, 4 H, $w_{\frac{1}{2}}$ = 67 Hz, *m*-CH_{Dipp}), 24.9 (bs, 12 H, $w_{\frac{1}{2}}$ = 76 Hz, CH(CH₃)₂), 14.2 (bs, 12 H, $w_{\frac{1}{2}}$ = 355 Hz, Si(CH₃)₂), -4.55 (s, 2 H, $w_{\frac{1}{2}}$ = 40 Hz,

$p\text{-CH}_3$), -16.4 (s, 4 H, $w_{\frac{1}{2}} = 61$ Hz, CH_{Ph}), -30.0 (bs, 12 H, $w_{\frac{1}{2}} = 700$ Hz, $\text{CH}(\text{CH}_3)_2$), -31.0 (s, 2 H, $w_{\frac{1}{2}} = 67$ Hz, $p\text{-CH}_{\text{Dipp}}$), -42.2 (bs, 4 H, $w_{\frac{1}{2}} = 640$ Hz, CH_{Ph}). Elemental analysis of $\text{C}_{40}\text{H}_{56}\text{CoN}_2\text{Si}_2$ (680.01 g mol $^{-1}$): calcd: N 4.12, C 70.65, H 8.30; found: N 4.29, C 70.25, H 8.15%. IR (ATR, cm $^{-1}$): $\tilde{\nu} = 3068$ (w), 3047 (w), 3014 (w), 2964 (m), 2950 (m), 2932 (m), 2867 (w), 1586 (w), 146 (w), 1450 (w), 1426 (m), 1382 (w), 1360 (w), 1311 (m), 1253 (m), 1236 (m), 1186 (m), 1107 (m), 1098 (m), 1051 (w), 1038 (w), 998 (w), 961 (w), 910 (s), 879 (m), 848 (s), 824 (s), 789 (vs), 767 (s), 734 (s), 699 (s), 650 (m), 588 (m), 534 (m), 474 (m), 439 (w), 424 (m), 412 (m). Evans (500.1 MHz, 300 K, C_6D_6 + 1% TMS): $\mu_{\text{eff}} = 4.89\mu_{\text{B}}$; $\mu_{\text{s.o.}} = 3.87\mu_{\text{B}}$.

K{18c6}[ML 1_2] (M = Mn–Co). One equivalent of [ML 1_2] (M = Mn–Co) and one equivalent of 18-crown-6 were dissolved in 5 mL of diethyl ether. After adding KCl_8 (1.1 equiv.) the reaction mixture was stirred for several minutes at room temperature, while a change in colour was observed (Mn: beige \rightarrow dark violet; Fe: orange \rightarrow red; Co: dark red \rightarrow light green). The graphite was filtered off, layered with *n*-pentane and cooled to -40 °C for several days for crystallization. The solution was decanted off and the remaining crystals were dried *in vacuo*. Crystalline K{18c6}[ML 1_2] (M = Mn–Co) was obtained in yields of 24–77%.

K{18c6}[MnL $^1L^1*$]. Using 56 mg of [MnL 1_2], K{18c6}[MnL $^1L^1*$] could be obtained as a dark violet crystalline solid. Yield: 20 mg (0.02 mmol, 24%). Crystals, suitable for X-ray diffraction analysis, were obtained from a *n*-pentane layered solution of K{18c6}[MnL $^1L^1*$] in Et $_2$ O at -40 °C. Elemental analysis of $\text{C}_{52}\text{H}_{80}\text{MnKN}_2\text{O}_6\text{Si}_2$ (979.43 g mol $^{-1}$): calcd: N 2.86, C 63.77, H 8.23; found: N 3.26, C 64.27, H 8.14%. IR (ATR, cm $^{-1}$): $\tilde{\nu} = 3060$ (w), 3039 (w), 3003 (w), 2951 (m), 2895 (m), 2861 (m), 1584 (w), 1454 (m), 1421 (s), 1377 (w), 1351 (m), 1312 (m), 1284 (w), 1237 (s), 1192 (m), 1104 (vs), 1039 (m), 961 (m), 926 (s), 881 (w), 823 (s), 782 (s), 770 (m), 749 (w), 736 (m), 725 (w), 700 (s), 680 (m), 641 (m), 618 (w), 584 (m), 530 (m), 503 (w), 475 (m), 434 (m). Evans (500.1 MHz, 300 K, THF- d_8 + 1% TMS): $\mu_{\text{eff}} = 5.37\mu_{\text{B}}$; $\mu_{\text{s.o.}} = 5.92\mu_{\text{B}}$.

K{18c6}[FeL 1_2]. Using 100 mg of [FeL 1_2], K{18c6}[FeL 1_2] could be obtained as a light green crystalline solid. Yield: 109 mg (0.11 mmol, 74%). Crystals, suitable for X-ray diffraction analysis, were obtained from a *n*-pentane layered solution of K{18c6}[FeL 1_2] in Et $_2$ O at -40 °C. ^1H NMR (300.2 MHz, THF- d_8 , 300 K, ppm): $\delta = 26.6$ (bs, $w_{\frac{1}{2}} = 480$ Hz), 25.9 (bs, $w_{\frac{1}{2}} = 610$ Hz), 12.9 (bs, 6 H, $w_{\frac{1}{2}} = 2070$ Hz, Si(CH $_3$) $_2$), 9.89 (bs, $w_{\frac{1}{2}} = 200$ Hz), 2.64 (s, 24 H, $w_{\frac{1}{2}} = 21.8$ Hz, 18c6), -7.68 (s, $w_{\frac{1}{2}} = 76$ Hz, CH_{Ph}), -12.8 (s, $w_{\frac{1}{2}} = 76$ Hz, CH_{Ph}), -54 (bs, $w_{\frac{1}{2}} = 3800$ Hz), -105.0 (bs, $w_{\frac{1}{2}} = 1400$ Hz, CH(CH $_3$) $_2$). Elemental analysis of $\text{C}_{52}\text{H}_{80}\text{FeKN}_2\text{O}_6\text{Si}_2$ (980.33 g mol $^{-1}$): calcd: N 2.86, C 63.71, H 8.23; found: N 3.34, C 63.30, H 8.15%. IR (ATR, cm $^{-1}$): $\tilde{\nu} = 3061$ (w), 3043 (w), 2951 (m), 3899 (m), 2860 (m), 1583 (w), 1472 (m), 1454 (m), 1420 (m), 1376 (w), 1351 (m), 1312 (m), 1284 (w), 1237 (s), 1193 (m), 1100 (vs), 1053 (m), 1040 (m), 997 (w), 962 (s), 925 (s), 883 (w), 866 (w), 834 (s), 866 (w), 834 (s), 804 (s), 781 (s), 727 (m), 702 (m), 685 (m), 671 (w), 640 (m), 621 (w), 583 (w), 531 (m), 476 (m), 430 (m). Evans (500.1 MHz, 300 K, THF- d_8 + 1% TMS): $\mu_{\text{eff}} = 4.52\mu_{\text{B}}$; $\mu_{\text{s.o.}} = 3.87\mu_{\text{B}}$.

K{18c6}[CoL 1_2]. Using 70 mg of [CoL 1_2], K{18c6}[CoL 1_2] could be obtained as a light green crystalline solid. Yield: 75 mg (0.08 mmol, 77%). Crystals, suitable for X-ray diffraction analysis, were obtained from a *n*-pentane layered solution of K{18c6}[CoL 1_2] in Et $_2$ O at -40 °C. ^1H NMR (300.2 MHz, THF- d_8 , 300 K, ppm): $\delta = 23.3$ (bs, 4 H, $w_{\frac{1}{2}} = 500$ Hz, CH(CH $_3$) $_2$), 21.4 (bs, 12 H, $w_{\frac{1}{2}} = 160$ Hz, Si(CH $_3$) $_2$), 17.0 (bs, 12 H, $w_{\frac{1}{2}} = 38$ Hz, CH(CH $_3$) $_2$), 14.6 (bs, 4 H, $w_{\frac{1}{2}} = 28$ Hz, *m*-CH $_{\text{Dipp}}$), 3.01 (s, 24 H, $w_{\frac{1}{2}} = 19.9$ Hz, 18c6), 2.85 (s, 2 H, $w_{\frac{1}{2}} = 15.5$ Hz, *p*-CH $_{\text{Dipp}}$), -2.59 (s, 2 H, $w_{\frac{1}{2}} = 14.8$ Hz, CH_{Ph}), -7.39 (s, 4 H, $w_{\frac{1}{2}} = 19.7$ Hz, CH_{Ph}), -38.1 (bs, 4 H, $w_{\frac{1}{2}} = 218$ Hz, CH_{Ph}), -84.9 (bs, 12 H, $w_{\frac{1}{2}} = 100$ Hz, CH(CH $_3$) $_2$). Elemental analysis of $\text{C}_{52}\text{H}_{80}\text{CoKN}_2\text{O}_6\text{Si}_2$ (983.42 g mol $^{-1}$): calcd: N 2.85, C 63.51, H 8.20; found: N 3.24, C 63.71, H 8.13%. IR (ATR, cm $^{-1}$): $\tilde{\nu} = 3060$ (w), 3045 (w), 2953 (m), 2913 (w), 2900 (w), 2859 (m), 1582 (w), 1475 (w), 1454 (m), 1420 (m), 1380 (w), 1351 (m), 1312 (m), 1284 (w), 1239 (m), 1196 (m), 1102 (vs), 1055 (m), 1039 (m), 992 (w), 961 (m), 933 (m), 830 (m), 803 (s), 780 (s), 760 (w), 741 (w), 727 (m), 702 (m), 668 (w), 640 (m), 588 (w), 540 (m), 533 (m), 478 (m), 436 (m). Evans (500.1 MHz, 300 K, THF- d_8 + 1% TMS): $\mu_{\text{eff}} = 3.94\mu_{\text{B}}$; $\mu_{\text{s.o.}} = 2.83\mu_{\text{B}}$.

$\text{-N}(\text{Dipp})\text{SiMePh}_2$ (L 2) containing compounds

HL 2 . 4.48 mL of 2,6-di-iso-propylaniline (24 mmol, 1 equiv.) were cooled to -20 °C in Et $_2$ O before adding 1 equivalent of *n*-BuLi (24 mmol, 1 equiv.) dropwise. It was stirred at room temperature for one hour before it was cooled to -20 °C, again. A precooled solution of 5.00 mL of chloro(dimethyl) phenyl silane (24 mmol, 1 equiv.) in Et $_2$ O was added slowly, whereas a light yellow solution and a colourless precipitate appeared. The reaction mixture was allowed to stir overnight at room temperature before the solvent was removed *in vacuo*. To extract the desired product, *n*-pentane was added and the white residue (LiCl) was filtered off afterwards. The solvent was removed *in vacuo* to obtain a colourless, viscous liquid (HL 2) in a yield of 99%. Yield: 8.89 g (0.024 mmol, 99%). ^1H NMR: (300.2 MHz, C_6D_6 , 300 K, ppm): $\delta = 7.56\text{--}7.59$ (m, 4 H, *m*-CH $_{\text{Ph}}$), 7.14–7.17* (m, 6 H, *o/p*-CH $_{\text{Ph}}$), 7.01–7.08 (m, 3 H, CH $_{\text{Dipp}}$), 3.37 (h, 2 H, $^3J_{\text{H,H}} = 6.86$ Hz, CH(CH $_3$) $_2$), 2.90 (bs, 1 H, NH), 1.04 (d, 12 H, $^3J_{\text{H,H}} = 6.84$ Hz, CH(CH $_3$) $_2$), 0.54 (s, 3 H, Si(CH $_3$)). $^{13}\text{C}\text{-}\{^1\text{H}\}$ NMR: (75.5 MHz, C_6D_6 , 300 K, ppm): $\delta = 143.7$ (s, NC $_{\text{ipso}}$), 139.4 (s, *o*-C $_{\text{Dipp}}$), 138.2 (s, SiC $_{\text{ipso}}$), 134.7 (s, *o*-CH $_{\text{Ph}}$), 129.8 (s, *p*-CH $_{\text{Ph}}$), 128.1 (s, *m*-CH $_{\text{Ph}}$), 124.1 (s, *p*-CH $_{\text{Dipp}}$), 123.5 (s, *m*-CH $_{\text{Dipp}}$), 28.8 (s, CH(CH $_3$) $_2$), 23.7 (s, CH(CH $_3$) $_2$), -2.63 (s, Si(CH $_3$)). *, The signal partially overlaps with the solvent signal.

LiL 2 . 3.00 g (8.03 mmol, 1 equiv.) of HL 2 were dissolved in 20 mL of *n*-pentane. It was cooled to -20 °C and *n*-BuLi (8.03 mmol, 1 equiv.) was added dropwise, while a white precipitate appeared immediately. After stirring for a further 30 minutes the solid was filtered off and washed with *n*-pentane before drying *in vacuo*. LiL 2 could be obtained as a white solid in a yield of 77%. Yield: 2.69 g (7.09 mmol, 88%). Crystals, suitable for X-ray diffraction analysis, were obtained from a *n*-pentane layered solution of LiL 2 in THF at -40 °C. ^1H NMR: (300.2 MHz, C_6D_6 , 300 K, ppm): $\delta = 7.49\text{--}7.52$ (dd, 4 H,

$^3J_{\text{H,H}} = 7.61$ Hz, $^3J_{\text{H,H}} = 1.80$ Hz, $m\text{-CH}_{\text{Ph}}$, 7.11–7.21* (m, 6 H, $o/p\text{-CH}_{\text{Ph}}$), 6.84–6.93 (m, 3 H, CH_{Dipp}), 3.09 (h, 2 H, $^3J_{\text{H,H}} = 6.84$ Hz, $\text{CH}(\text{CH}_3)_2$), 0.92 (d, 6 H, $^3J_{\text{H,H}} = 6.06$ Hz, $\text{CH}(\text{CH}_3)_2$), 0.61 (d, 6 H, $^3J_{\text{H,H}} = 6.46$ Hz, $\text{CH}(\text{CH}_3)_2$), 0.51 (s, 3 H, $\text{Si}(\text{CH}_3)_3$). *, The signal overlaps with the solvent signal. $^{13}\text{C}\{-^1\text{H}\}$ NMR: (75.5 MHz, C_6D_6 , 300 K, ppm): $\delta = 149.1$ (s, NC_{ipso}), 143.1 (s, SiC_{ipso}), 141.4 (s, $o\text{-C}_{\text{Dipp}}$), 134.8 (s, $o\text{-CH}_{\text{Ph}}$), 129.5 (s, $p\text{-CH}_{\text{Ph}}$), 129.0 (s, $m\text{-CH}_{\text{Ph}}$), 124.6 (s, $m\text{-CH}_{\text{Dipp}}$), 120.7 (s, $p\text{-CH}_{\text{Dipp}}$), 28.2 (s, $\text{CH}(\text{CH}_3)_2$), 25.2 (s, $\text{CH}(\text{CH}_3)_2$), 24.9 (s, $\text{CH}(\text{CH}_3)_2$), 1.96 (s, $\text{Si}(\text{CH}_3)_3$). ^1H NMR: (300.2 MHz, THF-d_8 , 300 K, ppm): $\delta = 7.48\text{--}7.51$ (m, 4 H, $m\text{-CH}_{\text{Ph}}$), 7.10–7.13 (m, 6 H, $o/p\text{-CH}_{\text{Ph}}$), 6.76 (d, 2 H, $^3J_{\text{H,H}} = 7.46$ Hz, $m\text{-PhH}$), 6.43 (t, 1 H, $^3J_{\text{H,H}} = 7.43$ Hz, $p\text{-PhH}$), 4.01 (h, $^3J_{\text{H,H}} = 6.90$ Hz, 2 H, $\text{CH}(\text{CH}_3)_2$), 0.93 (d, 12 H, $^3J_{\text{H,H}} = 6.90$ Hz, $\text{CH}(\text{CH}_3)_2$), 0.45 (s, 3 H, $\text{Si}(\text{CH}_3)_3$). $^{13}\text{C}\{-^1\text{H}\}$ NMR: (300.2 MHz, THF-d_8 , 300 K, ppm): $\delta = 156.4$ (s, NC_{ipso}), 147.1 (s, $o\text{-C}_{\text{Dipp}}$), 143.6 (s, SiC_{ipso}), 135.5 (s, $o\text{-CH}_{\text{Ph}}$), 127.6 (s, $p\text{-CH}_{\text{Ph}}$), 127.4 (s, $m\text{-CH}_{\text{Ph}}$), 122.7 (s, $m\text{-CH}_{\text{Dipp}}$), 115.8 (s, $p\text{-CH}_{\text{Dipp}}$), 27.6 (s, $\text{CH}(\text{CH}_3)_2$), 24.9* (s, $\text{CH}(\text{CH}_3)_2$), 2.45 (s, $\text{Si}(\text{CH}_3)_3$). *, The signal (partially) overlaps with the solvent signal. Elemental analysis of $\text{C}_{25}\text{H}_{30}\text{LiNSi}$ (379.55 g mol $^{-1}$): calcd: N 3.69, C 79.11, H 7.97; found: N 3.85, C 79.56, H 8.07%. IR (ATR, cm^{-1}): $\tilde{\nu} = 3065$ (w), 3048 (w), 2962 (w), 2949 (m), 2921 (w), 2899 (w), 2862 (m), 1587 (w), 1486 (w), 1455 (m), 1421 (s), 1384 (m), 1362 (w), 1339 (w), 1302 (m), 1248 (m), 1234 (s), 1187 (m), 1157 (w), 1145 (w), 1100 (s), 1067 (w), 1037 (m), 997 (w), 942 (s), 930 (s), 879 (w), 811 (m), 788 (s), 770 (s), 736 (s), 702 (vs), 672 (m), 645 (m), 618 (w), 600 (w), 577 (m), 530 (s), 480 (s), 453 (m), 422 (s).

$[\text{CrL}^2_2]$. 49 mg of CrCl_2 (0.40 mmol, 1 equiv.) and 300 mg of LiL^2 (0.56 mmol, 2 equiv.) were suspended in 15 mL of diethyl ether. It was stirred overnight at room temperature, while a change in colour to dark brown was observed. All volatiles were removed under reduced pressure before resolving the obtained residue in n -pentane. The lithium chloride was filtered off and it was cooled to -40 °C for crystallization. After several days, the solution was decanted off and the remaining orange crystals were dried *in vacuo*. Crystalline $[\text{CrL}^2_2]$ was obtained in a yield of 10%. **Yield:** 22 g (0.03 mmol, 10%). Elemental analysis of $\text{C}_{50}\text{H}_{60}\text{CrN}_2\text{Si}_2$ (797.21 g mol $^{-1}$): calcd: N 3.51, C 75.33, H 7.59; found: N 3.62, C 75.13, H 7.90%. IR (ATR, cm^{-1}): $\tilde{\nu} = 3064$ (w), 3047 (w), 2954 (m), 2925 (m), 2925 (m), 2863 (m), 1586 (w), 1483 (w), 1458 (m), 1424 (s), 1380 (w), 1359 (w), 1313 (m), 1252 (m), 1204 (m), 1184 (m), 1155 (w), 1142 (w), 1105 (s), 1041 (m), 996 (w), 951 (m), 893 (m), 873 (m), 854 (m), 824 (m), 812 (m), 787 (s), 766 (s), 734 (s), 698 (vs), 652 (m), 590 (m), 529 (m), 482 (s), 448 (m), 425 (m), 403 (w). Evans (500.1 MHz, 300 K, $\text{C}_6\text{D}_6 + 1\%$ TMS): $\mu_{\text{eff}} = 3.24\mu_{\text{B}}$; $\mu_{\text{S.O.}} = 4.89\mu_{\text{B}}$.

$-\text{N}(\text{Dipp})\text{SiPh}_3$ (L^3) containing compounds

HL^3 . The synthesis of these compounds was described in the literature *via* an alternative pathway with no analytical data.⁶⁶ 1.60 mL of 2,6-di-*iso*-propylaniline (8.50 mmol, 1 equiv.) was cooled to -20 °C in Et_2O before adding 1 equivalent of $n\text{-BuLi}$ (8.50 mmol) dropwise. It was stirred at room temperature for one hour before it was cooled to -20 °C,

again. A precooled solution of 2.51 mg of chlorotriphenylsilane (8.50 mmol, 1 equiv.) in Et_2O was added dropwise, whereas a light yellow solution and a colourless precipitate appeared. The reaction mixture was allowed to stir overnight at room temperature before the solution was filtered off and the residue was washed with n -pentane. After drying *in vacuo*, HL^3 could be obtained as a colourless oil in a yield of 97%. **Yield:** 3.63 g (8.34 mmol, 97%). Crystals, suitable for X-ray diffraction analysis, were obtained from a solution of HL^3 in n -pentane at -40 °C. ^1H NMR: (300.2 MHz, THF-d_8 , 300 K, ppm): $\delta = 7.46\text{--}7.48$ (m, 6 H, $m\text{-CH}_{\text{Ph}}$), 7.24–7.36 (m, 9 H, $o/p\text{-CH}_{\text{Ph}}$), 6.91 (m, 3 H, CH_{Dipp}), 4.05 (bs, 1 H, NH), 3.43 (h, $^3J_{\text{H,H}} = 6.64$ Hz, 2 H, $\text{CH}(\text{CH}_3)_2$), 0.83 (d, 12 H, $^3J_{\text{H,H}} = 6.84$ Hz, $\text{CH}(\text{CH}_3)_2$). $^{13}\text{C}\{-^1\text{H}\}$ NMR: (75.5 MHz, THF-d_8 , 300 K, ppm): $\delta = 145.9$ (s, NC_{ipso}), 139.8 (s, $o\text{-C}_{\text{Dipp}}$), 136.8 (s, SiC_{ipso}), 136.5 (s, $o\text{-CH}_{\text{Ph}}$), 130.2 (s, $p\text{-CH}_{\text{Ph}}$), 128.3 (s, $m\text{-CH}_{\text{Ph}}$), 124.6 (s, $p\text{-CH}_{\text{Dipp}}$), 123.5 (s, $m\text{-CH}_{\text{Dipp}}$), 29.2 (s, $\text{CH}(\text{CH}_3)_2$), 23.7 (s, $\text{CH}(\text{CH}_3)_2$).

LiL^3 . 3.35 g (7.69 mmol, 1 equiv.) of HL^3 were dissolved in 20 mL of Et_2O . It was cooled to -20 °C and $n\text{-BuLi}$ (7.69 mmol, 1 equiv.) was added dropwise, while a white precipitate appeared immediately. After stirring for a further 30 minutes, the solid was filtered off and washed with n -pentane before drying *in vacuo*. LiL^3 could be obtained as a white solid in a yield of 96%. **Yield:** 3.26 g (7.38 mmol, 96%). Crystals, suitable for X-ray diffraction analysis, were obtained from a n -pentane layered solution of LiL^3 in THF at -40 °C. ^1H NMR: (300.2 MHz, THF-d_8 , 300 K, ppm): $\delta = 7.41\text{--}7.44$ (m, 6 H, $m\text{-CH}_{\text{Ph}}$), 7.13–7.15 (m, 9 H, $o/p\text{-CH}_{\text{Ph}}$), 6.75 (d, 2 H, $^3J_{\text{H,H}} = 7.48$ Hz, $m\text{-CH}_{\text{Dipp}}$), 6.44 (t, 1 H, $^3J_{\text{H,H}} = 7.51$ Hz, $p\text{-CH}_{\text{Dipp}}$), 3.90 (h, 2 H, $^3J_{\text{H,H}} = 6.85$ Hz, $\text{CH}(\text{CH}_3)_2$), 0.77 (d, 12 H, $^3J_{\text{H,H}} = 6.69$ Hz, $\text{CH}(\text{CH}_3)_2$). $^{13}\text{C}\{-^1\text{H}\}$ NMR: (75.5 MHz, THF-d_8 , 300 K, ppm): $\delta = 155.4$ (s, NC_{ipso}), 144.8 (s, SiC_{ipso}), 143.5 (s, $o\text{-C}_{\text{Dipp}}$), 136.5 (s, $o\text{-CH}_{\text{Ph}}$), 128.0 (s, $p\text{-CH}_{\text{Ph}}$), 127.4 (s, $m\text{-CH}_{\text{Ph}}$), 122.8 (s, $m\text{-CH}_{\text{Dipp}}$), 116.2 (s, $p\text{-CH}_{\text{Dipp}}$), 28.0 (s, $\text{CH}(\text{CH}_3)_2$), 24.5 (s, $\text{CH}(\text{CH}_3)_2$). Elemental analysis of $\text{C}_{30}\text{H}_{32}\text{LiNSi}$ (441.62 g mol $^{-1}$): calcd: N 3.17, C 81.59, H 7.30; found: N 3.56, C 81.78, H 7.45%. IR (ATR, cm^{-1}): $\tilde{\nu} = 3060$ (w), 3043 (w), 2953 (m), 2881 (m), 2861 (m), 1584 (m), 1481 (w), 1458 (m), 1416 (s), 1375 (w), 1354 (w), 1336 (m), 1317 (m), 1275 (m), 1253 (s), 1205 (m), 1180 (w), 1152 (w), 1140 (w), 1098 (s), 1040 (s), 972 (w), 960 (m), 919 (m), 886 (m), 807 (w), 764 (m), 746 (s), 698 (vs), 675 (m), 652 (m), 617 (w), 594 (w), 572 (m), 528 (m), 497 (s), 442 (m), 424 (m).

$[\text{FeL}^3_2]$. 35 mg of FeCl_2 (0.28 mmol, 1 equiv.) and 350 mg of LiL^3 (0.56 mmol, 2 equiv.) were suspended in 15 mL of diethyl ether. It was stirred overnight at room temperature, while a change in colour from beige to yellowish green was observed. All volatiles were removed under reduced pressure before resolving the obtained residue in n -pentane. The lithium chloride was filtered off and it was cooled to -40 °C for crystallization. After several days, the solution was decanted off and the remaining orange crystals were dried *in vacuo*. Crystalline $[\text{FeL}^3_2]$ was obtained in a yield of 53%. **Yield:** 135 mg (0.14 mmol, 53%). Crystals, suitable for X-ray diffraction analysis, were obtained from a saturated n -pentane solution of $[\text{FeL}^3_2]$ at -40 °C. ^1H NMR (300.2 MHz, C_6D_6 , 300 K, ppm): $\delta =$

44.9 (bs, $\omega_{\frac{1}{2}} = 2310$ Hz), 42.0 (bs, $\omega_{\frac{1}{2}} = 230$ Hz), 18.7 (bs, $\omega_{\frac{1}{2}} = 930$ Hz), 14.5 (bs, $\omega_{\frac{1}{2}} = 860$ Hz), -3.90 (bs, $\omega_{\frac{1}{2}} = 200$ Hz), -10.3 (bs, $\omega_{\frac{1}{2}} = 180$ Hz), -27.0 (bs, $\omega_{\frac{1}{2}} = 360$ Hz), -32.6 (bs, $\omega_{\frac{1}{2}} = 530$ Hz), -41.7 (bs, $\omega_{\frac{1}{2}} = 430$ Hz). Elemental analysis of $C_6H_{64}FeN_2Si_2 \times C_4H_{10}O$ (999.32 g mol⁻¹): calcd: N 2.80, C 76.92, H 7.46; found: N 2.94, C 76.84, H 7.55% **IR** (ATR, cm⁻¹): $\tilde{\nu} = 3066$ (w), 3050 (w), 2958 (m), 2923 (w), 2863 (w), 1586 (w), 1482 (w), 1457 (w), 1426 (m), 1380 (w), 1359 (w), 1311 (m), 1254 (m), 1240 (m), 1185 (m), 1104 (s), 1040 (m), 996 (w), 908 (m), 878 (w), 829 (m), 788 (s), 737 (m), 697 (vs), 595 (m), 535 (m), 497 (vs), 444 (m), 429 (m), 408 (w). **Evans** (500.1 MHz, 300 K, C₆D₆ + 1% TMS): $\mu_{\text{eff}} = 4.88\mu_B$; $\mu_{\text{s.o.}} = 4.89\mu_B$.

K{18c6}[FeL³]₂. 30 mg of [FeL³]₂ (0.03 mmol, 1 equiv.) and 8.5 mg of 18-crown-6 (0.03 mmol, 1 equiv.) were dissolved in 5 mL of THF. After adding K₂C₈ (0.04 mmol, 1.1 equiv.) the reaction mixture was stirred for several minutes at room temperature, while a change in color from orange to dark red was observed. The graphite was filtered off before layering with *n*-pentane. It was allowed to crystallize at -40 °C for several days before the solution was decanted off. After washing with *n*-pentane the dark red crystals were dried *in vacuo*. Crystalline K{18c6}[FeL³]₂ was obtained in a yield of 31%. **Yield**: 12 mg (0.010 mmol, 31%). Crystals, suitable for X-ray diffraction analysis, were obtained from a *n*-pentane layered solution of [FeL³]₂⁻ in THF at -40 °C. **¹H NMR** (300.2 MHz, THF-*d*₈, 300 K, ppm): $\delta = 23.7$ (bs, $\omega_{\frac{1}{2}} = 740$ Hz), 20.4 (bs, $\omega_{\frac{1}{2}} = 670$ Hz), 2.97 (s, 24 H, $\omega_{\frac{1}{2}} = 25.5$ Hz, 18c6), -101.8 (bs, $\omega_{\frac{1}{2}} = 1360$ Hz). Elemental analysis of C₇₂H₈₈FeKN₂O₆Si₂ (1228.62 g mol⁻¹): calcd: N 2.28, C 70.39, H 7.22; found: N 2.51, C 70.72, H 7.33%. **IR** (ATR, cm⁻¹): $\tilde{\nu} = 3060$ (w), 3040 (w), 2951 (m), 2896 (m), 2859 (m), 1584 (w), 1564 (w), 1471 (m), 1454 (m), 1422 (s), 1376 (w), 1351 (m), 1313 (m), 1284 (w), 1241 (m), 1189 (m), 1100 (vs), 998 (w), 960 (m), 929 (m), 878 (w), 821 (m), 779 (s), 738 (m), 697 (vs), 593 (m), 533 (m), 501 (s), 443 (w), 427 (m), 415 (w). **Evans** (500.1 MHz, 300 K, THF-*d*₈ + 1% TMS): $\mu_{\text{eff}} = 4.60\mu_B$; $\mu_{\text{s.o.}} = 3.87\mu_B$.

-N(Dipp)SiMe₂(allyl) (L⁴) containing compounds

HL⁴. 2.79 mL of 2,6-di-iso-propylaniline (14.8 mmol, 1 equiv.) were cooled to -20 °C in Et₂O before adding 1 equivalent of *n*-BuLi (14.8 mmol) dropwise. It was stirred at room temperature for one hour before it was cooled to -20 °C, again. A precooled solution of 2.51 mg of chloro(dimethyl)allyl silane (14.8 mmol, 1 equiv.) in Et₂O was added slowly, whereas a colourless precipitate appeared. The reaction mixture was allowed to stir overnight at room temperature before the solvent was removed *in vacuo*. The desired product (**HL⁴**) was obtained after condensation of the remaining residue (80 °C, 10⁻³ mbar) as a colourless, viscous liquid in a yield of 86%. **Yield**: 3.49 g (12.7 mmol, 86%). **¹H NMR**: (300.2 MHz, C₆D₆, 300 K, ppm): $\delta = 7.16$ -7.23* (m, 3 H, *m/p*-CH_{Dipp}), 5.81-5.95 (m, 1 H, CH=CH₂), 4.99-5.05 (m, 2 H, CH=CH₂), 3.53 (h, 2 H, ³J_{H,H} = 6.80 Hz, CH(CH₃)₂), 2.23 (bs, 1 H, NH), 1.70 (d, 2 H, ³J_{H,H} = 7.78 Hz, SiCH₂), 1.27 (d, 12 H, ³J_{H,H} = 6.87 Hz, CH(CH₃)₂), 0.16 (s, 6 H, Si(CH₃)₂). *, The signal overlaps with the solvent signal. **¹³C-{¹H} NMR**: (75.5 MHz, C₆D₆, 300 K, ppm): δ

= 144.7 (s, NC_{ipso}), 139.5 (s, *o*-C_{Dipp}), 134.9 (s, CH=CH₂), 124.4 (s, *p*-CH_{Dipp}), 123.4 (s, *m*-CH_{Dipp}), 113.7 (s, CH=CH₂), 28.5 (s, CH(CH₃)₂), 26.2 (s, SiCH₂), 23.9 (s, CH(CH₃)₂), -1.26 (s, Si(CH₃)₂).

LiL⁴. 3.00 g (10.8 mmol, 1 equiv.) of **HL⁴** were dissolved in 20 mL of *n*-pentane. It was cooled to -20 °C and *n*-BuLi (10.8 mmol, 1 equiv.) was added dropwise, while a white precipitate appeared immediately. After stirring for a further 30 minutes, the solid was filtered off and washed with *n*-pentane before drying *in vacuo*. **LiL⁴** could be obtained as a white solid in a yield of 80%. **Yield**: 2.44 g (8.67 mmol, 80%). **¹H NMR**: (300.2 MHz, C₆D₆, 300 K, ppm): $\delta = 6.93$ (d, 2 H, ³J_{H,H} = 7.60 Hz, *m*-CH_{Dipp}), 6.83 (t, 1 H, ³J_{H,H} = 6.88 Hz, *p*-CH_{Dipp}), 6.08-6.25 (m, 1 H, CH=CH₂), 5.00-5.11 (m, 2 H, CH=CH₂), 3.25 (h, 2 H, ³J_{H,H} = 6.83 Hz, CH(CH₃)₂), 1.73 (d, 2 H, ³J_{H,H} = 8.08 Hz, SiCH₂), 1.17 (d, 6 H, ³J_{H,H} = 6.69 Hz, CH(CH₃)₂), 0.80 (d, 6 H, ³J_{H,H} = 6.64 Hz, CH(CH₃)₂), 0.18 (s, 6 H, Si(CH₃)₂). **¹³C-{¹H} NMR**: (75.5 MHz, C₆D₆, 300 K, ppm): $\delta = 150.2$ (NC_{ipso}), 143.0 (*o*-C_{Dipp}), 140.9 (CH=CH₂), 124.3 (*m*-CH_{Dipp}), 120.2 (*p*-CH_{Dipp}), 112.1 (CH=CH₂), 29.9 (SiCH₂), 27.9 (CH(CH₃)₂), 25.2 (CH(CH₃)₂), 24.9 (CH(CH₃)₂), 1.03 (Si(CH₃)₂). **¹H NMR**: (300.2 MHz, THF-*d*₈, 300 K, ppm): $\delta = 6.72$ (d, 2 H, ³J_{H,H} = 7.45 Hz, *m*-CH_{Dipp}), 6.35 (t, 1 H, ³J_{H,H} = 7.40 Hz, *p*-CH_{Dipp}), 5.75-5.90 (m, 1 H, CH=CH₂), 4.53-4.64 (m, 2 H, CH=CH₂), 4.03 (h, 2 H, ³J_{H,H} = 6.93 Hz, CH(CH₃)₂), 1.54 (d, 2 H, ³J_{H,H} = 8.27 Hz, SiCH₂), 1.05 (d, 12 H, ³J_{H,H} = 6.93 Hz, CH(CH₃)₂), -0.08 (s, 6 H, Si(CH₃)₂). **¹³C-{¹H} NMR**: (75.5 MHz, THF-*d*₈, 300 K, ppm): $\delta = 157.7$ (NC_{ipso}), 143.7 (*o*-C_{Dipp}), 141.0 (CH=CH₂), 122.4 (*m*-CH_{Dipp}), 115.2 (*p*-CH_{Dipp}), 109.2 (CH=CH₂), 30.8 (SiCH₂), 27.2 (CH(CH₃)₂), 1.87 (Si(CH₃)₂). *, The signal of the CH(CH₃)₂- group overlaps with the solvent signal. Elemental analysis of C₁₇H₂₈LiNSi (281.44 g mol⁻¹): calcd: N 4.98, C 72.55, H 10.03; found: N 5.29, C 72.25, H 10.13%. **IR** (ATR, cm⁻¹): $\tilde{\nu} = 3078$ (w), 3047 (w), 3007 (w), 2957 (m), 2867 (m), 1628 (m), 1617 (m), 1589 (w), 1457 (m), 1419 (s), 1385 (m), 1362 (m), 1305 (m), 1247 (s), 1229 (s), 1185 (s), 1142 (m), 1107 (m), 1038 (m), 1008 (w), 991 (w), 927 (vs), 897 (s), 819 (s), 783 (s), 768 (s), 744 (m), 723 (m), 690 (w), 663 (m), 631 (m), 578 (m), 559 (w), 528 (s), 453 (m), 435 (m).

[ML⁴]₂ (M = Cr-Co). One equivalent of MCl₂ (M = Cr-Co) and two equivalents of **LiL⁴** were suspended in 15 mL of diethyl ether. It was allowed to stir overnight at room temperature, while a change in colour was observed (Cr: green → dark green; Mn: beige → dark beige; Fe: brown → dark yellow; Co: light yellow → dark red-brown). All volatiles were removed under reduced pressure before resolving the obtained residue in *n*-pentane. The lithium chloride was filtered off and it was cooled to -40 °C for crystallization. After several days, the solution was decanted off and the obtained crystals were dried *in vacuo*. Crystalline **[ML⁴]₂** (M = Cr-Co) was obtained in yields of 47-78%.

[CrL⁴]₂. Using 109 mg of CrCl₂ (0.89 mmol, 1 equiv.), **[CrL⁴]₂** could be obtained as a dark green crystalline solid. **Yield**: 289 mg (0.48 mmol, 54%). Crystals, suitable for X-ray diffraction analysis, were obtained from a saturated *n*-pentane solution of **[CrL⁴]₂** at -40 °C. **¹H NMR** (300.2 MHz, C₆D₆, 300 K,

ppm): $\delta = 14.6$ (bs, $w_{\frac{1}{2}} = 940$ Hz), 9.5 (bs, $w_{\frac{1}{2}} = 380$ Hz), 6.0 (bs, $w_{\frac{1}{2}} = 460$ Hz), 3.3 (bs, $w_{\frac{1}{2}} = 1190$ Hz). Elemental analysis of $C_{34}H_{56}CrN_2Si_2$ (601.00 g mol⁻¹): calcd: N 4.66, C 67.95, H 9.39; found: N 5.03, C 67.88, H 8.91%. IR (ATR, cm⁻¹): $\tilde{\nu} = 3064$ (w), 3044 (w), 3009 (w), 2955 (m), 2929 (m), 2865 (m), 1587 (w), 1570 (m), 1460 (w), 1422 (m), 1380 (w), 1359 (w), 1307 (m), 1235 (s), 1194 (m), 1162 (w), 1142 (w), 1107 (s), 1052 (w), 1039 (w), 1002 (m), 923 (s), 891 (m), 825 (s), 772 (vs), 734 (m), 702 (w), 671 (m), 641 (m), 595 (m), 573 (w), 527 (m), 426 (m). Evans (500.1 MHz, 300 K, C₆D₆ + 1% TMS): $\mu_{\text{eff}} = 4.45\mu_B$; $\mu_{\text{s.o.}} = 4.89\mu_B$.

[MnL⁴₂]. Using 89 mg of MnCl₂ (0.71 mmol, 1 equiv.), [MnL⁴₂] could be obtained as a yellow crystalline solid. Yield: 203 mg (0.34 mmol, 47%). Crystals, suitable for X-ray diffraction analysis, were obtained from a saturated *n*-pentane solution of [MnL⁴₂] at -40 °C. ¹H NMR (300.2 MHz, C₆D₆, 300 K, ppm): $\delta = 30.8$ (bs, $w_{\frac{1}{2}} = 2100$ Hz), 11.9* (bs), -27.5 (bs, $w_{\frac{1}{2}} = 4300$ Hz). *, The half width could not be determined. Elemental analysis of $C_{34}H_{56}MnN_2Si_2$ (603.94 g mol⁻¹): calcd: N 4.64, C 67.62, H 9.35; found: N 4.91, C 67.15, H 9.07%. IR (ATR, cm⁻¹): $\tilde{\nu} = 3052$ (w), 2954 (m), 2902 (w), 2864 (m), 1592 (m), 1458 (m), 1424 (s), 1381 (w), 1358 (w), 1309 (m), 1254 (w), 1240 (s), 1195 (s), 1175 (w), 1154 (w), 1142 (w), 1104 (s), 1040 (m), 1025 (m), 926 (vs), 903 (m), 891 (s), 825 (s), 788 (s), 772 (s), 729 (m), 699 (m), 674 (m), 643 (m), 593 (m), 562 (m), 530 (m), 424 (m). Evans (500.1 MHz, 300 K, C₆D₆ + 1% TMS): $\mu_{\text{eff}} = 5.27\mu_B$; $\mu_{\text{s.o.}} = 5.92\mu_B$.

[FeL⁴₂]. Using 90 mg of FeCl₂ (0.71 mmol, 1 equiv.), [FeL⁴₂] could be obtained as a yellow crystalline solid. Yield: 293 mg (0.48 mmol, 68%). Crystals, suitable for X-ray diffraction analysis, were obtained from a saturated *n*-pentane solution of [FeL⁴₂] at -40 °C. ¹H NMR (300.2 MHz, C₆D₆, 300 K, ppm): $\delta = 157.6$ (bs, $w_{\frac{1}{2}} = 2250$ Hz, CH_{allyl}), 48.9 (s, 4 H, $w_{\frac{1}{2}} = 270$ Hz, *m*-CH_{Dipp}), 35.1 (bs, 4 H, $w_{\frac{1}{2}} = 1590$ Hz, CH(CH₃)₂), 24.0 (s, 12 H, $w_{\frac{1}{2}} = 335$ Hz, CH(CH₃)₂), 22.2 (bs, 12 H, $w_{\frac{1}{2}} = 666$ Hz, Si(CH₃)₂), 16.7 (bs, $w_{\frac{1}{2}} = 3400$ Hz, CH_{allyl}), -28.2 (s, 12 H, $w_{\frac{1}{2}} = 710$ Hz, CH(CH₃)₂), -37.5 (s, 2 H, $w_{\frac{1}{2}} = 150$ Hz, *p*-CH_{Dipp}), -135.2 (bs, $w_{\frac{1}{2}} = 2630$ Hz, CH_{allyl}). ¹H NMR (300.2 MHz, THF-*d*₈, 300 K, ppm): $\delta = 147.3$ (bs, $w_{\frac{1}{2}} = 1490$ Hz, CH_{allyl}), 49.2 (s, 4 H, $w_{\frac{1}{2}} = 160$ Hz, *m*-CH_{Dipp}), 34.0 (bs, 4 H, $w_{\frac{1}{2}} = 1200$ Hz, CH(CH₃)₂), 23.2 (s, 12 H, $w_{\frac{1}{2}} = 240$ Hz, CH(CH₃)₂), 20.2 (bs, 12 H, $w_{\frac{1}{2}} = 530$ Hz, Si(CH₃)₂), 15.5 (bs, $w_{\frac{1}{2}} = 2400$ Hz, CH_{allyl}), -31.3 (bs, 12 H, $w_{\frac{1}{2}} = 580$ Hz, CH(CH₃)₂), -37.1 (s, 2 H, $w_{\frac{1}{2}} = 110$ Hz, *p*-CH_{Dipp}), -121.5 (bs, $w_{\frac{1}{2}} = 3200$ Hz, CH_{allyl}). Elemental analysis of $C_{34}H_{56}FeN_2Si_2$ (604.85 g mol⁻¹): calcd: N 4.63, C 67.52, H 9.33; found: N 4.58, C 67.20, H 9.16%. IR (ATR, cm⁻¹): $\tilde{\nu} = 3051$ (w), 3012 (w), 2956 (m), 2901 (m), 2865 (m), 1577 (w), 1460 (m), 1424 (s), 1381 (w), 1359 (w), 1307 (m), 1255 (m), 1236 (s), 1191 (s), 1154 (w), 1142 (w), 1104 (s), 1053 (w), 1040 (m), 1005 (m), 952 (w), 917 (s), 885 (m), 826 (s), 787 (s), 774 (vs), 728 (m), 699 (m), 677 (m), 645 (m), 596 (m), 569 (m), 532 (m), 426 (m). Evans (500.1 MHz, 300 K, C₆D₆ + 1% TMS): $\mu_{\text{eff}} = 5.14\mu_B$; $\mu_{\text{s.o.}} = 4.89\mu_B$.

[CoL⁴₂]. Using 90 mg of CoCl₂ (0.71 mmol, 1 equiv.), [CoL⁴₂] could be obtained as a yellow crystalline solid. Yield: 335 mg (0.55 mmol, 78%). Crystals, suitable for X-ray diffraction ana-

lysis, were obtained from a saturated *n*-pentane solution of [CoL⁴₂] at -40 °C. ¹H NMR (300.2 MHz, C₆D₆, 300 K, ppm): $\delta = 57.1$ (bs, $w_{\frac{1}{2}} = 650$ Hz, CH_{allyl}), 56.1 (bs, 4 H, $w_{\frac{1}{2}} = 124$ Hz, *m*-CH_{Dipp}), 39.5 (bs, 12 H, $w_{\frac{1}{2}} = 141$ Hz, CH(CH₃)₂), 26.5 (bs, 12 H, $w_{\frac{1}{2}} = 420$ Hz, Si(CH₃)₂), -32.1 (s, 2 H, $w_{\frac{1}{2}} = 56$ Hz, *p*-CH_{Dipp}), -48 (bs, $w_{\frac{1}{2}} = 2740$ Hz, CH_{allyl}), -79.7 (bs, 12 H, $w_{\frac{1}{2}} = 390$ Hz, CH(CH₃)₂), -164 (bs, $w_{\frac{1}{2}} = 1780$ Hz, CH_{allyl}). ¹H NMR (300.2 MHz, THF-*d*₈, 300 K, ppm): $\delta = 59.2$ (bs, $w_{\frac{1}{2}} = 580$ Hz, CH_{allyl}), 53.2 (bs, 4 H, $w_{\frac{1}{2}} = 130$ Hz, *m*-CH_{Dipp}), 37.2 (bs, 12 H, $w_{\frac{1}{2}} = 160$ Hz, CH(CH₃)₂), 25.4 (bs, 12 H, $w_{\frac{1}{2}} = 470$ Hz, Si(CH₃)₂), -34.7 (s, 2 H, $w_{\frac{1}{2}} = 94$ Hz, *p*-CH_{Dipp}), -80.3 (bs, 12 H, $w_{\frac{1}{2}} = 440$ Hz, CH(CH₃)₂), -138.0 (bs, $w_{\frac{1}{2}} = 960$ Hz, CH_{allyl}), -192.6 (bs, $w_{\frac{1}{2}} = 1220$ Hz, CH_{allyl}). Elemental analysis of $C_{34}H_{56}CoN_2Si_2$ (607.94 g mol⁻¹): calcd: N 4.61, C 67.17, H 9.29; found: N 4.89, C 66.85, H 9.08%. IR (ATR, cm⁻¹): $\tilde{\nu} = 3060$ (w), 3011 (w), 2956 (m), 2927 (w), 2903 (w), 2865 (m), 1583 (m), 1463 (w), 1424 (s), 1381 (w), 1358 (w), 1307 (m), 1252 (m), 1238 (s), 1193 (s), 1142 (w), 1101 (s), 1051 (w), 1041 (w), 1101 (w), 1051 (w), 1041 (m), 1010 (w), 920 (vs), 886 (s), 826 (vs), 790 (s), 774 (vs), 730 (m), 697 (m), 676 (m), 647 (m), 595 (m), 567 (m), 532 (m), 426 (m). Evans (500.1 MHz, 300 K, C₆D₆ + 1% TMS): $\mu_{\text{eff}} = 4.84\mu_B$; $\mu_{\text{s.o.}} = 3.87\mu_B$.

(K{18c6})₂[CrL⁴₂]. Using 50 mg of [CrL⁴₂], (K{18c6})₂[CrL⁴₂]₂ could be obtained as a green crystalline solid. Yield: 32 mg (0.035 mmol, 44%). Crystals, suitable for X-ray diffraction analysis, were obtained from a *n*-pentane layered solution of (K{18c6})₂[CrL⁴₂]₂ in Et₂O at -40 °C. ¹H NMR (300.2 MHz, THF-*d*₈, 300 K, ppm): $\delta = 34.1$ (bs, $w_{\frac{1}{2}} = 1060$ Hz), 14.9 (bs, $w_{\frac{1}{2}} = 590$ Hz), 12.2 (bs, $w_{\frac{1}{2}} = 780$ Hz), 8.1 (bs, $w_{\frac{1}{2}} = 770$ Hz), 3.57* (s, 24 H, 18c6), -16.5 (bs, $w_{\frac{1}{2}} = 470$ Hz). *, The signal overlaps with the solvent signal. Elemental analysis of $C_{46}H_{80}CrKN_2O_6Si_2$ (904.42 g mol⁻¹): calcd: N 3.10, C 61.09, H 8.92; found: N 3.41, C 61.12, H 8.90%. IR (ATR, cm⁻¹): $\tilde{\nu} = 3036$ (w), 2950 (m), 2899 (m), 2860 (m), 1624 (w), 1583 (w), 1470 (w), 1454 (m), 1418 (m), 1376 (w), 1351 (m), 1314 (m), 1283 (w), 1244 (m), 1196 (m), 1172 (w), 1132 (m), 1103 (vs), 1054 (m), 1033 (m), 991 (w), 960 (m), 931 (m), 881 (w), 821 (s), 771 (s), 736 (m), 666 (m), 632 (m), 578 (m), 559 (w), 530 (m), 447 (m), 423 (m). Evans (500.1 MHz, 300 K, THF-*d*₈ + 1% TMS): $\mu_{\text{eff}} = 6.17\mu_B$; $\mu_{\text{s.o.}} = 6.93\mu_B$.

K{18c6}[CoL⁴₂]. Using 100 mg of [CoL⁴₂], K{18c6}[CoL⁴₂] could be obtained as a dark greenish brown crystalline solid. Yield: 97 mg (0.11 mmol, 65%). Crystals, suitable for X-ray diffraction analysis, were obtained from a *n*-pentane layered solution of K{18c6}[CoL⁴₂] in Et₂O at -40 °C. ¹H NMR (300.2 MHz, THF-*d*₈, 300 K, ppm): $\delta = 47.4$ (bs, $w_{\frac{1}{2}} = 220$ Hz, CH_{allyl}), 23.4 (bs, 2 H, $w_{\frac{1}{2}} = 320$ Hz, CH_{allyl}), 18.0 (s, 4 H, $w_{\frac{1}{2}} = 18.7$ Hz, *m*-CH_{Dipp}), 9.71 (bs, 2 H, $w_{\frac{1}{2}} = 180$ Hz, CH_{allyl}), 6.73 (s, 12 H, $w_{\frac{1}{2}} = 88$ Hz, Si(CH₃)₂), 4.57 (s, 12 H, $w_{\frac{1}{2}} = 20$ Hz, CH(CH₃)₂), 3.52 (s, 24 H, $w_{\frac{1}{2}} = 7.0$ Hz, 18c6), -3.34 (bs, 4 H, $w_{\frac{1}{2}} = 450$ Hz, CH(CH₃)₂), -4.84 (s, 2 H, $w_{\frac{1}{2}} = 17$ Hz, *p*-CH_{Dipp}), -31.7 (bs, 12 H, $w_{\frac{1}{2}} = 84$ Hz, CH(CH₃)₂), -53.8 (bs, 4 H, $w_{\frac{1}{2}} = 250$ Hz, CH_{allyl}). Elemental analysis of $C_{46}H_{80}CoKN_2O_6Si_2$ (911.36 g mol⁻¹): calcd: N 3.07, C 60.62, H 8.85; found: N 2.90, C 60.75, H 8.77%. IR (ATR, cm⁻¹): $\tilde{\nu} = 3031$ (w), 2954 (m), 2900 (m), 2861 (m), 1581 (w), 1461 (m), 1416 (m), 1377 (w), 1353 (w), 1311 (m), 1284 (w), 1243 (s), 1200 (m), 1101 (vs), 1053 (m),

1042 (m), 1008 (w), 956 (s), 898 (m), 821 (s), 769 (s), 729 (m), 700 (w), 659 (m), 604 (w), 572 (w), 519 (m), 428 (m). **Evans** (500.1 MHz, 300 K, THF-*d*₈ + 1% TMS): $\mu_{\text{eff}} = 4.04\mu_{\text{B}}$; $\mu_{\text{s.o.}} = 2.83\mu_{\text{B}}$.

Imido complexes

K{18c6}[Co(NDipp)L₂]. 48 mg of K{18c6}[CoL₂] (0.05 mmol, 1 equiv.) were dissolved in an Et₂O : THF mixture (1 : 1, v/v). Dipp azide (10 mg, 0.05 mmol, 1 equiv.) was added, while a spontaneous colour change from dark green to dark brown was observable. After allowing to crystallize at -40 °C for several days, the grown crystals were isolated and dried *in vacuo*. K{18c6}[Co(NDipp)L₂] was obtained as a dark green crystalline solid in a yield of 67%. **Yield**: 38 mg (0.03 mmol, 67%). ¹H NMR (300.2 MHz, THF-*d*₈, 300 K, ppm): $\delta = 117$ (bs, $w_{\frac{1}{2}} = 1500$ Hz), 66.2 (bs, $w_{\frac{1}{2}} = 1320$ Hz), 44.2 (bs, $w_{\frac{1}{2}} = 660$ Hz), 37.6 (bs, $w_{\frac{1}{2}} = 970$ Hz), 31.7 (bs, $w_{\frac{1}{2}} = 600$ Hz), 28.1 (bs, $w_{\frac{1}{2}} = 820$ Hz), 21.3 (bs, $w_{\frac{1}{2}} = 160$ Hz), 17.0 (s, $w_{\frac{1}{2}} = 36$ Hz), 14.6 (s, $w_{\frac{1}{2}} = 27$ Hz), 9.37 (bs, $w_{\frac{1}{2}} = 560$ Hz), 7.61 (s, $w_{\frac{1}{2}} = 14$ Hz), 7.25 (s, $w_{\frac{1}{2}} = 26$ Hz), 6.92 (s, $w_{\frac{1}{2}} = 66$ Hz), 3.67 (s, 24 H, $w_{\frac{1}{2}} = 6.4$ Hz, 18c6), 3.61 (s, $w_{\frac{1}{2}} = 9.1$ Hz, THF_{coord.}), 2.86 (s, $w_{\frac{1}{2}} = 23$ Hz), 1.77 (s, $w_{\frac{1}{2}} = 9.9$ Hz, THF_{coord.}), -1.93 (bs, $w_{\frac{1}{2}} = 1300$ Hz), -2.62 (s, $w_{\frac{1}{2}} = 13$ Hz), -7.43 (s, $w_{\frac{1}{2}} = 18$ Hz), -14.5 (bs, $w_{\frac{1}{2}} = 180$ Hz), -18.0 (bs, $w_{\frac{1}{2}} = 700$ Hz), -31.8 (bs, $w_{\frac{1}{2}} = 140$ Hz), -38.1 (bs, $w_{\frac{1}{2}} = 160$ Hz), -84.9 (bs, $w_{\frac{1}{2}} = 94$ Hz). Elemental analysis of C₆₄H₉₇CoKN₃O₆Si₂ (1158.70 g mol⁻¹): calcd: N 3.63, C 66.34, H 8.44; found: N 3.61, C 65.71, H 8.57%. **IR** (ATR, cm⁻¹): $\tilde{\nu} = 3065$ (w), 3053 (w), 3039 (w), 2948 (m), 2897 (m), 2860 (m), 2827 (w), 2791 (w), 1584 (w), 1469 (w), 1454 (m), 1421 (s), 1391 (w), 1376 (w), 1350 (m), 1312 (m), 1282 (w), 1237 (s), 1192 (m), 1103 (vs), 1055 (m), 960 (s), 931 (m), 908 (m), 883 (w), 831 (s), 802 (s), 767 (s), 741 (m), 726 (w), 701 (s), 683 (m), 651 (m), 576 (w), 541 (m), 528 (m), 477 (m), 431 (m). **Evans** (500.1 MHz, 300 K, THF-*d*₈ + 1% TMS): $\mu_{\text{eff}} = 4.87\mu_{\text{B}}$; $\mu_{\text{s.o.}} = 4.89\mu_{\text{B}}$.

K{18c6}[Co(NDipp)L₂]. 45 mg of K{18c6}[CoL₂] (0.05 mmol, 1 equiv.) were dissolved in an Et₂O : THF mixture (1 : 1, v/v). Dipp azide (10 mg, 0.05 mmol, 1 equiv.) was added to the above mixture, while a spontaneous colour change from dark green to dark brown was observable. After allowing to crystallize at -40 °C for several days, the grown crystals were isolated and dried *in vacuo*. K{18c6}[Co(NDipp)L₂] was obtained as a dark red crystalline solid in a yield of 54%. **Yield**: 29 mg (0.03 mmol, 65%). ¹H NMR (300.2 MHz, THF-*d*₈, 300 K, ppm): $\delta = 84.7$ (bs, $w_{\frac{1}{2}} = 300$ Hz), 30.5 (bs, $w_{\frac{1}{2}} = 680$ Hz), 26.2 (bs, $w_{\frac{1}{2}} = 780$ Hz), 7.1 (bs, $w_{\frac{1}{2}} = 130$ Hz), 4.42 (s, 24 H, $w_{\frac{1}{2}} = 12$ Hz, 18c6), 3.61 (s, 8 H, $w_{\frac{1}{2}} = 9.1$ Hz, THF_{coord.}), 1.77 (s, 8 H, $w_{\frac{1}{2}} = 8.2$ Hz, THF_{coord.}), -25.1 (bs, $w_{\frac{1}{2}} = 150$ Hz), -26.1 (s, $w_{\frac{1}{2}} = 190$ Hz), -52.4 (bs, $w_{\frac{1}{2}} = 18$ Hz), -53.4 (bs, $w_{\frac{1}{2}} = 15$ Hz). Elemental analysis of C₅₈H₉₇CoKN₃O₆Si₂ (1086.63 g mol⁻¹): calcd: N 3.87, C 64.11, H 9.00; found: N 3.80, C 63.68, H 8.84%. **IR** (ATR, cm⁻¹): $\tilde{\nu} = 3067$ (w), 3049 (w), 3025 (w), 2951 (m), 2897 (m), 2862 (m), 1624 (m), 1584 (w), 1456 (m), 1421 (s), 1392 (w), 1377 (w), 1351 (m), 1337 (w), 1311 (m), 1283 (w), 1236 (s), 1188 (m), 1132 (w), 1104 (vs), 1054 (m), 1037 (w), 993 (w), 961 (m), 930 (w), 903 (s), 878 (m), 835 (s), 799 (s), 782 (m), 739 (m), 705 (w), 675 (m), 646 (m), 585 (w), 556 (m), 537 (m),

437 (m). **Evans** (500.1 MHz, 300 K, THF-*d*₈ + 1% TMS): $\mu_{\text{eff}} = 5.05\mu_{\text{B}}$; $\mu_{\text{s.o.}} = 4.89\mu_{\text{B}}$.

X-ray diffraction analysis

Data for compounds LiL² (CCDC 2073681†), LiL³_b (CCDC 2073682†), [FeL₂] (CCDC 2074225†), [CoL₂] (CCDC 2074223†), K{18c6}[CoL₂] (CCDC 2074226†), [FeL₂] (CCDC 2074224†), K{18c6}[FeL₂] (CCDC 2074234†), [CrL₂] (CCDC 2074229†), [FeL₂] (CCDC 2074232†), [CoL₂] (CCDC 2074236†), (K{18c6})₂[CrL₂]₂ (CCDC 2074256†) and K{18c6}[Co(NDipp)L₂] (CCDC 2074231†) were collected at 100 K on a Bruker Quest D8 diffractometer (Bruker Corporation, Billerica, USA) using Incoatec Microfocus Source Mo-K α radiation and equipped with an Oxford Instrument Cooler Device (Oxford Instruments, Abingdon, UK) and a Photon 100 detector. Data for compound K{18c6}[MnL¹*L] (CCDC 2074317†) were collected at 100 K on an STOE Stadivari diffractometer using Cu-K α radiation and a DECTRIS Pilatus R 300 K detector. Data for compounds LiL¹ (CCDC 2073679†), HL³ (CCDC 2073678†), LiL³_a (CCDC 2073680†), K{18c6}[FeL₂] (CCDC 2074235†) and [MnL₂] (CCDC 2074233†) were collected at 100 K on an STOE IPDS2 diffractometer (STOE & Cie GmbH, Darmstadt, Germany) and data for compounds [MnL₂] (CCDC 2074237†), [CrL₂] (CCDC 2074230†), K{18c6}[CoL₂] (CCDC 2074228†) and K{18c6}[Co(NDipp)L₂] (CCDC 2074227†) were collected at 100 K on an STOE IPDS2T diffractometer using graphite-monochromated Mo-K α radiation ($\lambda = 0.71073$ Å) and equipped with an Oxford Instrument Cooler Device (Oxford Instruments, Abingdon, UK). The structures have been solved using OLEX SHELXT V2014/1⁶⁷ and refined by means of least-squares procedures on F² with the aid of the program SHELXL-2016/6⁶⁸ included in the software package WinGX version 1.63⁶⁹ or using CRYSTALS.⁷⁰ In the case of [CoL₂], the structure was refined using olex2.refine. The atomic scattering factors were taken from International Tables for X-ray Crystallography.⁷¹ All non-hydrogen atoms were refined anisotropically. All hydrogen atoms were refined by using a riding model. Disorders were found for LiL² (a coordinating THF molecule), LiL³_a (a coordinating THF molecule), LiL³_b (coordinating THF molecules), K{18c6}[MnL¹*L] (all atoms), K{18c6}[FeL₂] (two phenyl rings and two iso-propyl groups), K{18c6}[CoL₂] (methyl group), [CrL₂] (SiMePh₂ fragment), [FeL₂] (a free *n*-pentane molecule), K{18c6}[FeL₂] (a coordinated THF molecule and a free *n*-pentane molecule), (K{18c6})₂[CrL₂]₂ (crown ether, coordinated THF molecules, iso-propyl and allyl groups), K{18c6}[Co(NDipp)L₂] (a coordinated THF molecule) and K{18c6}[Co(NDipp)L₂] (coordinated THF molecules, allyl groups) and were modelled accordingly. The structures of [MnL₂], K{18c6}[MnL¹*L] and K{18c6}[FeL₂] were refined as inversion twins. For (K{18c6})₂[CrL₂]₂ weakly diffracting crystals and intrinsic crystallographic flaws could not be overcome despite multiple attempts. Absorption corrections were introduced by using the MULTISCAN and X-Red programs.⁷² Drawings of molecules are performed using the DIAMOND program (Crystal Impact, Bonn, Germany) with 50% probability displacement ellipsoids for non-H atoms. Additional details are given in the ESI.†

Author contributions

The manuscript was written through contributions of all authors. All authors have given approval to the final version of the manuscript.

Conflicts of interest

There are no conflicts to declare.

Acknowledgements

Special thanks to Dr Sergei Ivlev for helping with some of the crystallographic problems. C. G. W. thanks the Deutsche Forschungsgemeinschaft (grant WE 5627/4-1) and the Philipps-University for financial support.

Notes and references

- 1 P. P. Power, *Chem. Rev.*, 2012, **112**, 3482–3507.
- 2 D. L. Kays, *Dalton Trans.*, 2011, **40**, 769–778.
- 3 (a) S. Roy, K. C. Mondal and H. W. Roesky, *Acc. Chem. Res.*, 2016, **49**, 357–369; (b) P. C. Bunting, M. Atanasov, E. Damgaard-Møller, M. Perfetti, I. Crassee, M. Orlita, J. Overgaard, J. van Slageren, F. Neese and J. R. Long, *Science*, 2018, **362**(6421), eaat7319; (c) R. J. Witzke and T. D. Tilley, *Chem. Commun.*, 2019, **55**, 6559–6562; (d) M. I. Lipschutz, T. Chantarojsiri, Y. Dong and T. D. Tilley, *J. Am. Chem. Soc.*, 2015, **137**, 6366–6372; (e) A. M. Bryan, C.-Y. Lin, M. Sorai, Y. Miyazaki, H. M. Hoyt, A. Hablutzel, A. LaPointe, W. M. Reiff, P. P. Power and C. E. Schulz, *Inorg. Chem.*, 2014, **53**, 12100–12107; (f) J. Du, L. Wang, M. Xie and L. Deng, *Angew. Chem., Int. Ed.*, 2015, **54**, 12640–12644; (g) C. A. Laskowski, D. J. Bungum, S. M. Baldwin, S. A. Del Ciello, V. M. Iluc and G. L. Hillhouse, *J. Am. Chem. Soc.*, 2013, **135**, 18272–18275; (h) G. Ung and J. C. Peters, *Angew. Chem., Int. Ed.*, 2015, **54**, 532–535; (i) C. G. Werncke, P. C. Bunting, C. Duhayon, J. R. Long, S. Bontemps and S. Sabo-Etienne, *Angew. Chem., Int. Ed.*, 2015, **54**, 245–248; (j) M. I. Lipschutz and T. D. Tilley, *Angew. Chem., Int. Ed.*, 2014, **53**, 7290–7294; (k) J. N. Boynton, W. A. Merrill, W. M. Reiff, J. C. Fettinger and P. P. Power, *Inorg. Chem.*, 2012, **51**, 3212–3219; (l) C. L. Wagner, L. Tao, E. J. Thompson, T. A. Stich, J. Guo, J. C. Fettinger, L. A. Berben, R. D. Britt, S. Nagase and P. P. Power, *Angew. Chem., Int. Ed.*, 2016, **55**, 10444–10447; (m) H. Lei, J.-D. Guo, J. C. Fettinger, S. Nagase and P. P. Power, *J. Am. Chem. Soc.*, 2010, **132**, 17399–17401; (n) C. Schneider, S. Demeshko, F. Meyer and C. G. Werncke, *Chem. – Eur. J.*, 2021, **27**, 6348–6353.
- 4 K. Freitag, C. R. Stennett, A. Mansikkamäki, R. A. Fischer and P. P. Power, *Inorg. Chem.*, 2021, **60**, 4108–4115.
- 5 J. M. Zadrozny, D. J. Xiao, M. Atanasov, G. J. Long, F. Grandjean, F. Neese and J. R. Long, *Nat. Chem.*, 2013, **5**, 577–581.
- 6 A. M. Bryan, G. J. Long, F. Grandjean and P. P. Power, *Inorg. Chem.*, 2014, **53**, 2692–2698.
- 7 C. G. Werncke, E. Sutura, P. C. Bunting, L. Vendier, J. R. Long, M. Atanasov, F. Neese, S. Sabo-Etienne and S. Bontemps, *Chem. – Eur. J.*, 2016, **22**, 1668–1674.
- 8 H. R. Sharpe, A. M. Geer, L. J. Taylor, B. M. Gridley, T. J. Blundell, A. J. Blake, E. S. Davies, W. Lewis, J. McMaster, D. Robinson and D. L. Kays, *Nat. Commun.*, 2018, **9**, 3757.
- 9 C. Ni, T. A. Stich, G. J. Long and P. P. Power, *Chem. Commun.*, 2010, **46**, 4466.
- 10 C.-Y. Lin, J. C. Fettinger, N. F. Chilton, A. Formanuk, F. Grandjean, G. J. Long and P. P. Power, *Chem. Commun.*, 2015, **51**, 13275–13278.
- 11 (a) A. E. Ashley, A. R. Cowley, J. C. Green, D. R. Johnston, D. J. Watkin and D. L. Kays, *Eur. J. Inorg. Chem.*, 2009, **2009**, 2547–2552; (b) H. Chen, R. A. Bartlett, M. M. Olmstead, P. P. Power and S. C. Shoner, *J. Am. Chem. Soc.*, 1990, **112**, 1048–1055; (c) H. Chen, R. A. Bartlett, H. V. R. Dias, M. M. Olmstead and P. P. Power, *J. Am. Chem. Soc.*, 1989, **111**, 4338–4345; (d) R. A. Bartlett and P. P. Power, *J. Am. Chem. Soc.*, 1987, **109**, 7563–7564.
- 12 W. M. Reiff, C. E. Schulz, M.-H. Whangbo, J. I. Seo, Y. S. Lee, G. R. Potratz, C. W. Spicer and G. S. Girolami, *J. Am. Chem. Soc.*, 2009, **131**, 404–405.
- 13 C. Ni and P. P. Power, *Chem. Commun.*, 2009, 5543–5545.
- 14 T. Nguyen, A. Panda, M. M. Olmstead, A. F. Richards, M. Stender, M. Brynda and P. P. Power, *J. Am. Chem. Soc.*, 2005, **127**, 8545–8552.
- 15 J. J. Ellison, K. Ruhlandt-Senge and P. P. Power, *Angew. Chem., Int. Ed. Engl.*, 1994, **33**, 1178–1180.
- 16 D. L. Kays and A. R. Cowley, *Chem. Commun.*, 2007, 1053–1055.
- 17 (a) R. A. Andersen, K. Faegri, J. C. Green, A. Haaland, M. F. Lappert, W. P. Leung and K. Rypdal, *Inorg. Chem.*, 1988, **27**, 1782–1786; (b) B. D. Murray and P. P. Power, *Inorg. Chem.*, 1984, **23**, 4584–4588; (c) D. C. Bradley, M. B. Hursthouse, K. M. A. Malik and R. Möseler, *Transition Met. Chem.*, 1978, **3**, 253–254; (d) T. Deschner, K. W. Törnroos and R. Anwender, *Inorg. Chem.*, 2011, **50**, 7217–7228; (e) G. A. Sigel, R. A. Bartlett, D. Decker, M. M. Olmstead and P. P. Power, *Inorg. Chem.*, 1987, **26**, 1773–1780; (f) M. M. Olmstead, P. P. Power and S. C. Shoner, *Inorg. Chem.*, 1991, **30**, 2547–2551; (g) B. D. Murray, H. Hope and P. P. Power, *J. Am. Chem. Soc.*, 1985, **107**, 169–173; (h) P. P. Power and S. C. Shoner, *Angew. Chem., Int. Ed. Engl.*, 1991, **30**, 330–332.
- 18 R. Wolf, C. Ni, T. Nguyen, M. Brynda, G. J. Long, A. D. Sutton, R. C. Fischer, J. C. Fettinger, M. Hellman, L. Pu and P. P. Power, *Inorg. Chem.*, 2007, **46**, 11277–11290.
- 19 C. Ni, B. D. Ellis, T. A. Stich, J. C. Fettinger, G. J. Long, R. D. Britt and P. P. Power, *Dalton Trans.*, 2009, 5401.
- 20 A. M. Bryan, W. A. Merrill, W. M. Reiff, J. C. Fettinger and P. P. Power, *Inorg. Chem.*, 2012, **51**, 3366–3373.

- 21 I. C. Cai, M. S. Ziegler, P. C. Bunting, A. Nicolay, D. S. Levine, V. Kalendra, P. W. Smith, K. V. Lakshmi and T. D. Tilley, *Organometallics*, 2019, **38**, 1648–1663.
- 22 M. Atanasov, J. M. Zadrozny, J. R. Long and F. Neese, *Chem. Sci.*, 2013, **4**, 139–156.
- 23 W. M. Reiff, A. M. LaPointe and E. H. Witten, *J. Am. Chem. Soc.*, 2004, **126**, 10206–10207.
- 24 W. A. Merrill, T. A. Stich, M. Brynda, G. J. Yeagle, J. C. Fettinger, R. D. Hont, W. M. Reiff, C. E. Schulz, R. D. Britt and P. P. Power, *J. Am. Chem. Soc.*, 2009, **131**, 12693–12702.
- 25 C. A. Laskowski, G. R. Morello, C. T. Saouma, T. R. Cundari and G. L. Hillhouse, *Chem. Sci.*, 2013, **4**, 170–174.
- 26 (a) D. D. Beattie, E. G. Bowes, M. W. Drover, J. A. Love and L. L. Schafer, *Angew. Chem., Int. Ed.*, 2016, **55**, 13290–13295; (b) J. Hicks and C. Jones, *Organometallics*, 2015, **34**, 2118–2121.
- 27 S. N. König, D. Schneider, C. Maichle-Mössmer, B. M. Day, R. A. Layfield and R. Anwander, *Eur. J. Inorg. Chem.*, 2014, **2014**, 4302–4309.
- 28 (a) Z. Ouyang, J. Du, L. Wang, J. L. Kneebone, M. L. Neidig and L. Deng, *Inorg. Chem.*, 2015, **54**, 8808–8816; (b) Z. Ouyang, Y. Meng, J. Cheng, J. Xiao, S. Gao and L. Deng, *Organometallics*, 2016, **35**, 1361–1367.
- 29 I. C. Cai, M. I. Lipschutz and T. D. Tilley, *Chem. Commun.*, 2014, **50**, 13062–13065.
- 30 M. I. Lipschutz, X. Yang, R. Chatterjee and T. D. Tilley, *J. Am. Chem. Soc.*, 2013, **135**, 15298–15301.
- 31 C.-Y. Lin, J. C. Fettinger, F. Grandjean, G. J. Long and P. P. Power, *Inorg. Chem.*, 2014, **53**, 9400–9406.
- 32 C. G. Werncke and I. Müller, *Chem. Commun.*, 2020, **56**, 2268–2271.
- 33 (a) C. G. Werncke, L. Vendier, S. Sabo-Etienne, J.-P. Sutter, C. Pichon and S. Bontemps, *Eur. J. Inorg. Chem.*, 2017, **2017**, 1041–1406; (b) A. M. Bryan, G. J. Long, F. Grandjean and P. P. Power, *Inorg. Chem.*, 2013, **52**, 12152–12160; (c) R. T. Baker, J. C. Gordon, C. W. Hamilton, N. J. Henson, P.-H. Lin, S. Maguire, M. Murugesu, B. L. Scott and N. C. Smythe, *J. Am. Chem. Soc.*, 2012, **134**, 5598–5609; (d) R. A. Layfield, J. J. W. McDouall, M. Scheer, C. Schwarzmaier and F. Tuna, *Chem. Commun.*, 2011, **47**, 10623–10625; (e) A. Massard, P. Braunstein, A. A. Danopoulos, S. Choua and P. Rabu, *Organometallics*, 2015, **34**, 2429–2438; (f) N.-J. H. Kneusels, J. E. Münzer, K. Flosdorf, D. Jiang, B. Neumüller, L. Zhao, A. Eichhöfer, G. Frenking and I. Kuzu, *Dalton Trans.*, 2020, **49**, 2537–2546.
- 34 C.-Y. Lin, J. C. Fettinger and P. P. Power, *Inorg. Chem.*, 2017, **56**, 9892–9902.
- 35 (a) C. G. Werncke, J. Pfeiffer, I. Müller, L. Vendier, S. Sabo-Etienne and S. Bontemps, *Dalton Trans.*, 2019, **48**, 1757–1765; (b) I. Müller, C. Schneider, C. Pietzonka, F. Kraus and C. G. Werncke, *Inorganics*, 2019, **7**, 117; (c) I. Müller and C. G. Werncke, *Chem. – Eur. J.*, 2021, **27**, 4932–4938.
- 36 R. Weller, I. Müller, C. Duhayon, S. Sabo-Etienne, S. Bontemps and C. G. Werncke, *Dalton Trans.*, 2021, **50**, 4890–4903.
- 37 A. Reckziegel, M. Kour, B. Batistella, S. Mebs, K. Beuthert, R. Berger and G. Werncke, *Angew. Chem., Int. Ed.*, 2021, **60**, 15376–15380.
- 38 A. Reckziegel, C. Pietzonka, F. Kraus and C. G. Werncke, *Angew. Chem., Int. Ed.*, 2020, **59**, 8527–8531.
- 39 J. Wang, R. Liu, W. Ruan, Y. Li, K. C. Mondal, H. W. Roesky and H. Zhu, *Organometallics*, 2014, **33**, 2696–2703.
- 40 M. A. Petrie, K. Ruhlandt-Senge and P. P. Power, *Inorg. Chem.*, 1993, **32**, 1135–1141.
- 41 X. Wang, J. Li, S. Chen, W. Liu, Q. Ye and H. Zhu, *Dalton Trans.*, 2016, **45**, 6709–6717.
- 42 D. Braga, F. Grepioni, K. Biradha and G. R. Desiraju, *J. Chem. Soc., Dalton Trans.*, 1996, 3925.
- 43 C.-Y. Lin, J.-D. Guo, J. C. Fettinger, S. Nagase, F. Grandjean, G. J. Long, N. F. Chilton and P. P. Power, *Inorg. Chem.*, 2013, **52**, 13584–13593.
- 44 J. M. Zadrozny, M. Atanasov, A. M. Bryan, C.-Y. Lin, B. D. Rekker, P. P. Power, F. Neese and J. R. Long, *Chem. Sci.*, 2013, **4**, 125–138.
- 45 C. L. Wagner, L. Tao, J. C. Fettinger, R. D. Britt and P. P. Power, *Inorg. Chem.*, 2019, **58**, 8793–8799.
- 46 H.-J. Liu, I. C. Cai, A. Fedorov, M. S. Ziegler, C. Copéret and T. D. Tilley, *Helv. Chim. Acta*, 2016, **99**, 859–867.
- 47 I. Müller, D. Munz and C. G. Werncke, *Inorg. Chem.*, 2020, **59**, 9521–9537.
- 48 P. Betz, P. W. Jolly, C. Krueger and U. Zakrzewski, *Organometallics*, 1991, **10**, 3520–3525.
- 49 C. Lichtenberg, M. Adelhardt, M. Wörle, T. Büttner, K. Meyer and H. Grützmacher, *Organometallics*, 2015, **34**, 3079–3089.
- 50 C. Lichtenberg, L. Viciu, M. Adelhardt, J. Sutter, K. Meyer, B. de Bruin and H. Grützmacher, *Angew. Chem., Int. Ed.*, 2015, **54**, 5766–5771.
- 51 L. Wang, L. Hu, H. Zhang, H. Chen and L. Deng, *J. Am. Chem. Soc.*, 2015, **137**, 14196–14207.
- 52 A. Cutler, D. Ehnholt, P. Lennon, K. Nicholas, D. F. Marten, M. Madhavarao, S. Raghu, A. Rosan and M. Rosenblum, *J. Am. Chem. Soc.*, 1975, **97**, 3149–3157.
- 53 T. Chen, S. Jiang and E. Turos, *Tetrahedron Lett.*, 1994, **35**, 8325–8328.
- 54 B. J. Barrett and V. M. Iluc, *Inorg. Chem.*, 2014, **53**, 7248–7259.
- 55 Y. Tian, T. Maulbetsch, R. Jordan, K. W. Törnroos and D. Kunz, *Organometallics*, 2020, **39**, 1221–1229.
- 56 J. B. Lambert, C. L. Stern, Y. Zhao, W. C. Tse, C. E. Shawl, K. T. Lentz and L. Kania, *J. Organomet. Chem.*, 1998, **568**, 21–31.
- 57 K. Thum, A. Friedrich, J. Pahl, H. Elsen, J. Langer and S. Harder, *Chemistry*, 2021, **27**, 2513–2522.
- 58 (a) S. Deblon, L. Liesum, J. Harmer, H. Schönberg, A. Schweiger and H. Grützmacher, *Chem. – Eur. J.*, 2002, **8**, 601–611; (b) C. Chan, A. E. Carpenter, M. Gembicky, C. E. Moore, A. L. Rheingold and J. S. Figueroa, *Organometallics*, 2019, **38**, 1436–1444; (c) S. Asghar, S. B. Taylor, D. Elorriaga and R. B. Bedford, *Angew. Chem., Int. Ed.*, 2017, **56**, 16367–16370; (d) S. Pelties, T. Maier,

- D. Herrmann, B. de Bruin, C. Rebreyend, S. Gärtner, I. G. Shenderovich and R. Wolf, *Chem. – Eur. J.*, 2017, **23**, 6094–6102.
- 59 J. C. Ott, H. Wadepohl and L. H. Gade, *Inorg. Chem.*, 2021, **60**, 3927–3938.
- 60 (a) H. Lund, *J. Electrochem. Soc.*, 2002, **149**, S21; (b) J. H. P. Utley, T. Fanghänel, I. Grenthe, W. R. Salaneck, R. Sillanpää, G. Bernáth, J. Szúnyog and B. Långström, *Acta Chem. Scand.*, 1998, **52**, 237–249.
- 61 D. F. Evans, *J. Chem. Soc.*, 1959, 2003.
- 62 E. M. Schubert, *J. Chem. Educ.*, 1992, **69**, 62.
- 63 (a) T. A. Betley and J. C. Peters, *J. Am. Chem. Soc.*, 2003, **125**, 10782–10783; (b) X. Hu and K. Meyer, *J. Am. Chem. Soc.*, 2004, **126**, 16322–16323; (c) E. R. King, G. T. Sazama and T. A. Betley, *J. Am. Chem. Soc.*, 2012, **134**, 17858–17861; (d) D. M. Jenkins, T. A. Betley and J. C. Peters, *J. Am. Chem. Soc.*, 2002, **124**, 11238–11239; (e) X. Dai, P. Kapoor and T. H. Warren, *J. Am. Chem. Soc.*, 2004, **126**, 4798–4799; (f) C. Jones, C. Schulten, R. P. Rose, A. Stasch, S. Aldridge, W. D. Woodul, K. S. Murray, B. Moubaraki, M. Brynda, G. La Macchia and L. Gagliardi, *Angew. Chem., Int. Ed.*, 2009, **48**, 7406–7410; (g) Y. Liu, J. Du and L. Deng, *Inorg. Chem.*, 2017, **56**, 8278–8286; (h) S. Aghazada, D. Fehn, F. W. Heinemann, D. Munz and K. Meyer, *Angew. Chem., Int. Ed.*, 2021, **60**, 16480–16486; (i) P. J. Chirik, Y. Park, S. P. Semproni and H. Zhong, *Angew. Chem., Int. Ed.*, 2021, **60**, 14376–14380.
- 64 M. J. T. Wilding, D. A. Iovan and T. A. Betley, *J. Am. Chem. Soc.*, 2017, **139**, 12043–12049.
- 65 (a) G. Coin, R. Patra, S. Rana, J. P. Biswas, P. Dubourdeaux, M. Clémancey, S. P. de Visser, D. Maiti, P. Maldivi and J.-M. Latour, *ACS Catal.*, 2020, **10**, 10010–10020; (b) K. Ray, F. Heims and F. F. Pfaff, *Eur. J. Inorg. Chem.*, 2013, **2013**, 3784–3807; (c) P. F. Kuijpers, J. I. van der Vlugt, S. Schneider and B. de Bruin, *Chem. – Eur. J.*, 2017, **23**, 13819–13829.
- 66 S. Anga, Y. Sarazin, J.-F. Carpentier and T. K. Panda, *ChemCatChem*, 2016, **8**, 1373–1378.
- 67 O. V. Dolomanov, L. J. Bourhis, R. J. Gildea, J. Howard and H. Puschmann, *J. Appl. Crystallogr.*, 2009, **42**, 339–341.
- 68 G. M. Sheldrick, *Acta Crystallogr., Sect. C: Struct. Chem.*, 2015, **71**, 3–8.
- 69 L. J. Farrugia, *J. Appl. Crystallogr.*, 1999, **32**, 837–838.
- 70 P. W. Betteridge, J. R. Carruthers, R. I. Cooper, K. Prout and D. J. Watkin, *J. Appl. Crystallogr.*, 2003, **36**, 1487.
- 71 C. P. Brock, E. Arnold, M. I. Aroyo, A. Authier, G. Chapuis, Th. Hahn, S. R. Hall, D. M. Himmel, V. Kopský, D. B. Litvin, B. McMahon, U. Müller, E. Prince, M. G. Rossmann, U. Shmueli, T. R. Welberry and H. Wondratschek, *International tables for crystallography*, International Union of Crystallography, Springer, Chester, England, New York, 1st edn, 2006.
- 72 (a) *SADABS-2016/2*, Bruker, 2016; (b) X.-R. , *X-Area*, STOE, 2016.